AMERICAN COLLEGE OF VETERINARY RADIOLOGY

2010 Annual Scientific Meeting

August 15 - 19, 2010

GROVE PARK INN
ASHEVILLE, NORTH CAROLINA

PROGRAM COMMITTEE
Liz Watson, Program Chair
Jay Stefanacci, Program Co-Chair (ACVR Forum)
Ben Young, Program Co-Chair (Image Interpretation Session)
Mary K. Klein, Program Co-Chair, (Radiation Oncology)
Lorrie Gaschen, President Ultrasound Society
Federica Morandi, President Society of Veterinary Nuclear Medicine
John Hathcock, President CT/MRI Society
Norm Rantanen, President Large Animal Diagnostic Imaging Society
Jessica Winger, ACVR Meeting Manager
Susie Wilson, ACVR Administrator

ACVR ADMINISTRATION
Marti Larson, President
Val Samii, President – elect
Rob McLear, Treasurer
Tom Nyland, Webmaster/Secretary
Bill Brawner, President Radiation Oncology
Robert D. Pechman, Executive Director
Darryl N. Biery, Assistant Executive Director

Table of Contents

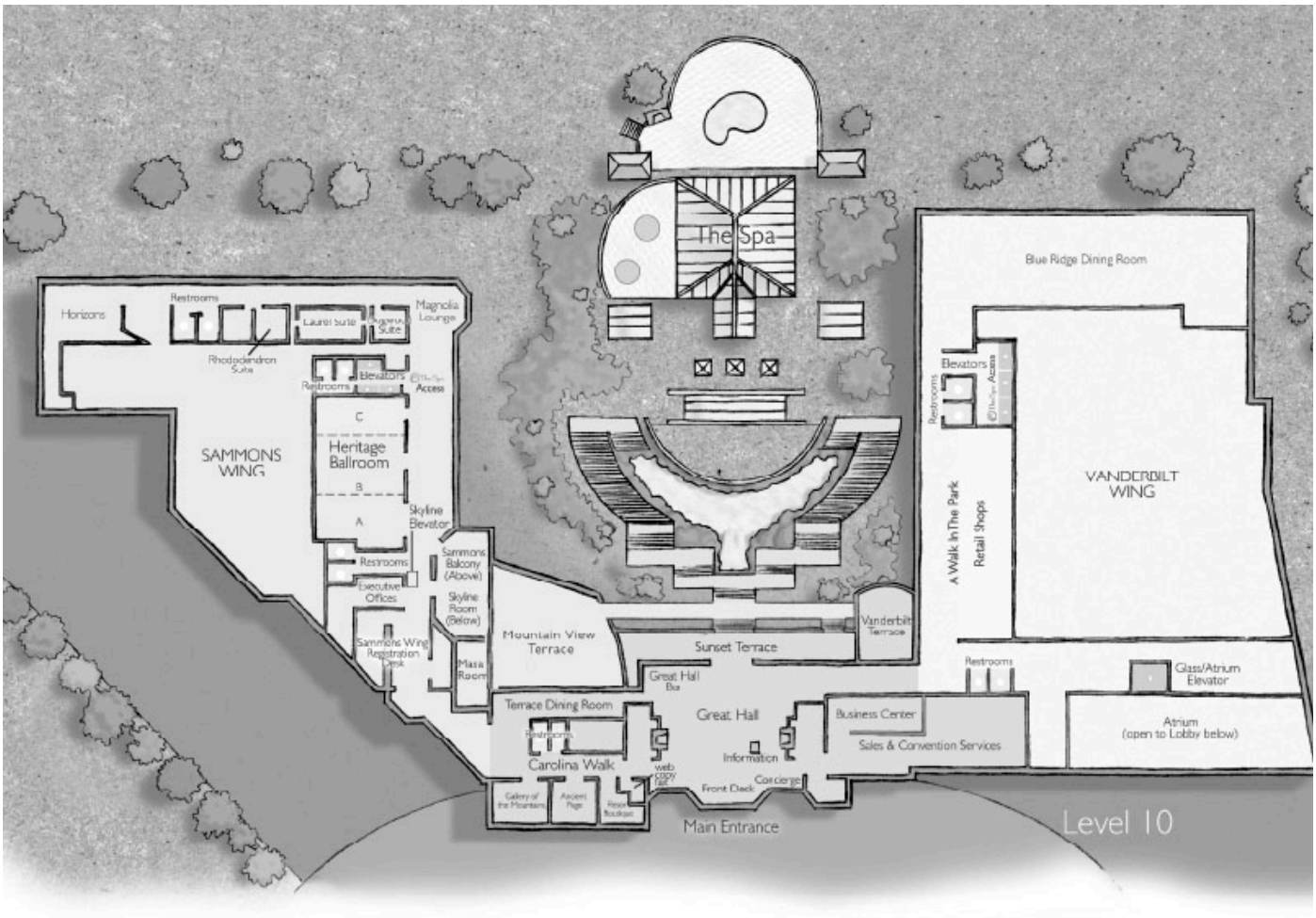

Guest Rooms

Main Inn

All three digit rooms are located in the Main Inn.

Sammons Wing

All rooms ending with the numbers 11-44 are located in the Sammons Wing.

Vanderbilt Wing

All rooms ending with the numbers 50-77 are located in the Vanderbilt Wing.

Elaine's

Take the Atrium elevator in the Vanderbilt Wing.

Meeting Rooms

All meeting rooms are located on the lobby level and the eighth floor.

Sammons Wing

Heritage Ballroom
Laurel Suite
Skyline Room
Dogwood Suite
Rhododendron Suite
Masa Room

Vanderbilt Wing

<u>Presidents (Level 8)</u>

Coolidge Suite
Roosevelt Suite
Wilson Suite
Hoover Suite
Taft Suite
Eisenhower Suite

The Grand Ballroom

THE AMERICAN COLLEGE OF VETERINARY RADIOLOGY GRATEFULLY ACKNOWLEDGES THE SUPPORT OF THE FOLLOWING COMPANIES AND WISHES TO THANK THEM FOR THEIR CONTRIBUTIONS

ADVANCED VETERINARY TECHNOLOGIES, INC.

PO Box 4099
New Windsor, NY 12553
Website: www.avtmri.com

Advanced Veterinary Technologies, Inc. is the only company dedicated to the design, engineering and manufacturing of MRI and X-Ray equipment specifically for use by veterinarians. Following the novel concept of Animal-Conscious Technology™ (ACT) - Technology Designed with the Veterinary Patient in Mind, AVT supplies veterinarians with the most advanced diagnostic options available, and pays special attention to patient safety and comfort, and to the quality and efficiency of the veterinary practice. AVT works within the existing cost parameters of veterinary care through use of simplified manufacturing processes and site preparation, and regular maintenance. This commitment to economy makes AVT's products available to a large number of veterinary environments including specialty hospitals, teaching institutions, private practices and regional imaging centers.

ALOKA ULTRASOUND

10 Fairfield Boulevard
Wallingford, CT 06942
Email: inquiry@aloka.com
Web: www.alokavet.com

ALOKA has a full range of ultrasound systems for most veterinary applications. The super premium Alpha 7 offers superb image quality for the most challenging cases. We also offer cost effective solutions in the SSD-3500 and SSD-4000. Our two portables, the SSD-500 and SSD-900 are reliable, rugged systems that are ideal for large animal reproduction, equine tendons and, with the 500, food animal live carcass evaluation. With the addition of the Sonosite family of battery operated lightweight systems, Aloka can now provide a system so portable you can carry it in a briefcase.

ASTERIS

PO Box 285-4 West Road
Stephentown, NY 12168
Website: www.asteris.biz

ASTERIS is an innovative, progressive corporation focusing on technology solutions for the veterinary industry. Founded in 2004, ASTERIS delivers inimitable PACS (Picture Archiving and Communication Systems) solutions and a groundbreaking veterinary information communication platform. A revolutionary concept, ASTERIS Veterinary Communication Network (VCN) enables veterinary practices, universities, and clients to access and share the full breadth of patient medical data at any time, from anywhere in the world.

BIOSOUND ESAOTE

8000 Castleway Drive
Indianapolis, IN 46250
Website: www.biosound.com

Biosound Esaote, an industry leader in diagnostic portable and console-based ultrasound systems, offers the MyLab® series, a high-performance ultrasound family. Offering systems that provide comprehensive diagnoses, feature high-level functionality and offer excellent value, the MyLab ultrasound line supplies flexible configurations to meet the specific needs of any Veterinary practice. Biosound Esaote has recently partnered with Vetel Diagnostics as its ultrasound distributor in the Veterinary market.

CANON (VIRTUAL IMAGING, INC.)

720 S. Powerline Road, Suite E
Deerfield Beach, FL 33442
Website: www.virtualimaging-fl.com

Virtual Imaging, Inc. is a wholly owned subsidiary of Canon U.S.A., Inc. Combining unmatched experience, extensive resources and broad business functions, Virtual Imaging collaborates with large complex hospital and government organizations as well as imaging centers and private physician offices to support them in becoming efficient, high-performance healthcare providers and professionals. Recently, Virtual Imaging has broadened its capabilities and solutions to channel the same business acumen to veterinary practices and organizational groups for the better treatment and care of animals. We assist in the advancement of our clients forward thinking goals, from strategic planning to day-to-day operations, with our commitment to provide products and services for diagnostic equipment, imaging solutions, and digital flat panel technology. With over 130 employees, 50+ Service Engineers, 55+ dealers nationwide and a proven track record; Virtual Imaging is able to combine the necessary expertise, skills and technologies that facilitate healthcare and veterinary providers to better diagnose diseases and treat conditions.

ELSEVIER

P.O. Box 360446
Birmingham, Al 35236
Email: d.camy@elsevier.com

SAUNDERS, MOSBY, CHURCHILL LIVINGSTONE, BUTTERWORTH HEINEMANN AND HANLEY BELFUS, a combined premier worldwide health science publishing company, now under the umbrella of ELSEVIER, INC., proudly presents our latest titles. Come visit us at our booth and browse through our complete selection of publications including books, periodicals and software. ELSEVIER, INC.: building insights, breaking boundaries.

FOVEA DR

P.O. Box 1908
1233 N. Ashley
Nixa, MO 65714
Toll Free: 888-368-3201
Website: www.FoveaDR.com

Fovea Direct Digital Radiography has reset the bar in veterinary x-ray. The entire line of Fovea systems has been designed and built from the ground up to be truly digital. Fovea offers the highest resolution and the fastest DR, with the lowest dose available. Cutting-edge technology, top-of-the-line equipment, and the ability to look ahead and anticipate the demands of veterinarians and their practices have helped cement Fovea's position as the industry leader. Fovea DR provides factory direct pricing, installation and a friendly support staff from our facility in America's heartland.

FUJIFILM MEDICAL SYSTEMS USA

419 West Avenue
Stamford, CT 06902-6300
Website: www.fujiprivatepractice.com

FUJIFILM Medical Systems USA, the world leader in digital x-ray systems, will showcase its latest system for veterinary practices the FDR D-evo--a portable flat panel detector that lets you convert any analog or CR room to DR. Fujifilm's portfolio also includes the FCR Prima, FCR XL-2 and FCR XC-2 systems which provide Fujifilm's high image quality, proven image optimization tools, and throughputs of up to 94 images per hour. Systems for viewing, archiving and storing digital x-rays are also available.

IDEXX DIGITAL IMAGING

One Idexx Drive
Westbrook, ME 04092

IDEXX Digital Imaging- to meet the diverse needs of any veterinary practice, IDEXX offers a full range of digital imaging solutions that were developed in conjunction with independent, board certified veterinary radiologists specifically for veterinary use. The IDEXX-DR™ 1417 and IDEXX-CR™ 1417 Digital Imaging systems can help your practice increase revenue, eliminate film associated expenses and improve productivity by streamlining workflow, in addition to increasing your diagnostic capabilities. Both systems offer complete integration through IDEXX SmartLink™ Digital Imaging with IDEXX Cornerstone® so you can get information where you need it, when you need it.

INNOVET

2901 W. Lawrence Avenue
Chicago, IL 60625
Website: www.innovet4vets.com/

InnoVet pioneered veterinary radiography in 1991 with the first x-ray system designed by veterinarians for veterinarians. This revolutionary unit combined all the tools needed for an x-ray exam into one compact package. Prior to this time, vets were relegated to use human medical x-ray systems for the unique needs of veterinary imaging. Ten years later, InnoVet will reshape the veterinary radiography market once more with the all-new Versa and Versa DR systems.

KINGSBRIDGE VETERINARIAN EQUIPMENT TECHNOLOGY SOLUTIONS

PO Box 297
Fontana, WI 53125
Website: www.kingsbridgeVETS.com

Kingsbridge Veterinarian Equipment Technology Solutions (KVETS) is the premier provider of refurbished CT, MRI, Ultrasound and other high technology imaging equipment serving the veterinary market. Our meticulous refurbishment process insures that every KVETS product meets the highest standards of performance and quality. Each KVETS product carries a full one year warranty and equipment service contracts are available.

ONCONCEPTS, LLC

24 Revella Street
Rochester, NY 14609

Onconcepts was founded with the primary goal of improving cancer care through efficient, high quality products that meet the needs of the Radiation Oncology environment. The three founders have 40 years combined clinical, technical and service expertise. One of our premium products is the Kodak 2000RT, the only simulation/portal CR system to offer Oncology specific software and a Beam Dosimetry Imaging Package. The future of Onconcepts includes new and innovative Radiation Oncology Imaging and QA products.

MEDICAL IMAGING TECHNOLOGIES (MIT)

261 Quality Drive
Thomson, GA 30824
Website: www.mit-tech.com

MIT (Medical Imaging Technologies) is a sales and service organization that specializes in providing equipment solutions to the world of veterinary diagnostic imaging. With state of the art refurbishing facilities near Augusta, Georgia and regional sales offices in the southeast, MIT has provided service to the industry since 1987. MIT provides permanent and temporary equipment solutions for CT, MR, Post-Processing Workstations, Traditional X-ray, Direct Digital Radiography Panels, and Ultrasound. Our service department employs factory trained engineers who specialize in the various modalities we sell. With our extensive knowledge base, the professionals at MIT bring a value proposition to your business which provides for the purchase of new technology at greatly reduced costs. Please visit us on-line at http://www.mit-tech.com for further information.

SOUND-EKLIN

5817 Dryden Place, Suite 101
Carlsbad, CA 92008

Sound-Eklin is the industry's uncontested leader in veterinary imaging including digital radiography ultrasound, imaging data management, viewing, and advanced imaging tools. Sound-Eklin is driving the industry forward with a commitment to open standards supported by strength, synergy and freedom of choice.

TGM^2

15375 Roosevelt Boulevard, Suite 300
Clearwater, FL 33760
Website: www.tgm2.com

TGM^2 was formed to provide accessory product services to the health care industry. We specialize in diagnostic imaging and radiation oncology equipment procurement including equipment room layout, installation and facility planning.

UNIVERSAL MEDICAL SYSTEMS

29500 Aurora Road, Unit 16
Solon, OH 44139
Email: sales@universal-systems.com
Website: www.veterinary-imaging.com

Universal Medical Systems, Inc. of Ohio is the only authorized distributor serving the veterinary market selling CT and MRI scanners directly from the major manufacturers designed specifically to meet your needs. New or certified systems are available with a variety of financing and service options. Visit us today and see for yourself how we scan every animal in less than 30 seconds.

UNIVERSAL ULTRASOUND

299 Adams Street
Bedford Hill, NY 10507
Email: ccarducci@UniversalUltrasound.com
Website: www.universalultrasound.com

Universal Ultrasound has partnered with over 10,000 veterinarians to bring veterinary imaging into their practices confidently and affordably. Universal offers a variety of packages for both beginning and advanced users, featuring all digital technology, portability, veterinary specific applications, complete connectivity and comprehensive training.

VETEL DIAGNOSTICS

4850 Davenport Creek Road
San Luis Obispo, CA 93401
Email: info@veteldiagnostics.com
Website: www.veteldiagnostics.com

VETEL Diagnostics offers veterinarians advanced diagnostic technologies including Envision, Explorer and Empower Digital Radiography Systems. Vetel's digital radiography systems were developed specifically for veterinarians with a focus on intuitive, user-friendly software and excellent image quality. System models include multiple companion animal configurations with a variety of panel sizes, available installed in a table or in a rugged portable case. Vetel's DR systems have the widest dynamic range available and are complete imaging systems with multiple image algorithms per view, image enhancement tools, accurate measurement tools and easy report generation. FLIR thermal imaging systems are revolutionizing veterinary medicine helping to diagnose difficult cases. Thermography applications include lameness diagnostics, pre-purchase exams, saddle fit evaluation and back pain detection.

VETERINARY INFORMATION NETWORK (VIN)

777 W. Covell Boulevard
Davis, CA 95616
Website: www.VIN.com

The Veterinary Information Network (VIN) is the premier online community, continuing education, and information resource for veterinarians. Founded in 1991, VIN reaches over 44,000 veterinarians, veterinary students, and industry partners worldwide. VIN is the leader in unlimited access to medical, product and practice management information.

VET RAY TECHNOLOGY BY SEDECAL

2920 N. Arlington Hts. Road
Arlington Heights, IL 60004
Website: www.vetray.com

Vetray Technology by Sedecal is the premium worldwide manufacturer of Veterinary Specific X-ray produces. Vetray Technology by Sedecal manufactures the largest line of High Frequency X-ray products for every Veterinary X-ray application. Small Animal: the highest quality table systems for Film or Digital. Equine: Single and Dual Overhead Tube Crane systems, Mobile and Portable systems.

American College of Veterinary Radiology

Special Thanks to the following Corporate Partners:

2010 Conference Bag Sponsor
CoActiv PACS 4 Vets

Badge Neck Lanyard Sponsor
Vetel Diagnostics

Cyber Café
Veterinary Information Network (VIN)

ACVR Reception Sponsors
Orthopedic Foundation for Animals
Universal Medical Systems, Inc.

ACVR Image Interpretation Session Sponsors
Fovea DR
Idexx
Sedecal
Sound-Eklin

Program Overview

2010 ACVR Scientific Meeting
August 15 – 19, 2010
Grove Park Inn
Asheville, North Carolina

Sunday, August 15, 2010

3:30 pm – 6:30 pm	*Registration opens*	Vanderbilt Registration

Monday, August 16, 2010

7:00 am	*Registration opens*	Vanderbilt Registration
7:00 am	Veterinary Ultrasound Society Meeting	Grand Ballroom A
8:00 am	ACVR Forum **How to Succeed in This Business: A Career Choice Seminar for Radiologists** Introduction: Dr. Jay Stefanacci	
8:10 am	Radiologists in the Military Dr. Cathy Banfield	
8:38 am	Radiologists in Industry/Corporate America Dr. Bill Hornof	
9:06 am	Radiologists in Academia Dr. Wil Mai	
9:34 am	Radiologists as Sole Proprietors: Mobile Ultrasound,Teleradiography Dr. Sloane Dupree	
10:02 am	*Break with Exhibitors*	Grand Ballroom B
10:12 am	Radiologists as Sole Proprietors: Large Animal (Equine) Dr. Norm Rantanen	
10:40 am	Radiologists as Sole Proprietors: Consultative Services, Teleradiography Dr. Matt Wright	
11:08 am	Discussion and Questions	
12:00 pm	*Buffet Lunch*	Grand Ballroom C

Monday, August 16, 2010, continued

1:00 pm	**Conference Welcome** Dr. Liz Watson, 2010 Program Chair	Grand Ballroom A
1:05 pm	**ACVR Presidential Address** Dr. Marti Larson	
1:35 pm	ACVR Keynote Address **Medical Imaging in the Digital Age: Facing Unexpected Challenges** Dr. Elizabeth Krupinski	
3:05 pm	*Break with Exhibitors*	Grand Ballroom B
3:30 pm	**ACVR Scientific Session 1: General Radiology**	
4:30 pm	*Adjourn for the day*	
5:00 pm	Opportunity to Meet Resident Coordinators	Grand Ballroom A
6:30 pm	*Welcome Reception*	The Vanderbilt Terrace

Tuesday, August 17, 2010 (*ACVR and RO simultaneous sessions)*

ACVR

7:00 am	*Registration opens*	Vanderbilt Registration
7:00 am	Society of Veterinary Nuclear Medicine Meeting	Grand Ballroom A
8:00 am	Ultrasound Society Keynote Address **Panel on Ultrasound Contrast**	
9:30 am	*Break with Exhibitors*	Grand Ballroom B
9:40 am	**ACVR Scientific Session 2: Ultrasound**	
10:40 am	*Break with Exhibitors*	Grand Ballroom B
11:00 am	**ACVR Scientific Session 3: Ultrasound**	
12:00 pm	*Box Lunch*	The Vanderbilt Terrace
1:00 pm	Group trip to the Biltmore	Pickup- Vanderbilt Wing, Level 10
5:00 pm	*Return*	

RO

7:00 am	*Registration opens*	Vanderbilt Registration
7:00 am	VRTOG Meeting	Roosevelt KL
8:00 am	Radiation Oncology Keynote Address **Time, Dose, Fractionation** Dr. Colin Orton	
9:30 am	**Radiation Oncology Scientific Session 1**	
10:06 am	*Break with Exhibitors*	Grand Ballroom B
10:36 am	**Radiation Oncology Scientific Session 2**	
12:00 pm	*Box Lunch*	The Vanderbilt Terrace
1:00 pm	Group trip to the Biltmore	Pickup- Vanderbilt Wing, Level 10
5:00 pm	*Return*	

Wednesday, August 18, 2010 (*ACVR and RO simultaneous sessions*)

ACVR

7:15 am	*Registration opens*	Vanderbilt Registration
7:15 am	CT/MRI Society meeting	Grand Ballroom A
8:15 am	Nuclear Medicine Keynote Address **Molecular Imaging: Technology, Tracers and Translation** Dr. Jon Wall	
9:45 am	*Break with Exhibitors*	Grand Ballroom B
10:00 am	**ACVR Scientific Session 4: Nuclear Medicine**	
10:48 am	*Break with Exhibitors*	Grand Ballroom B
11:12 am	**ACVR Scientific Session 5: Nuclear Medicine & General Radiology**	
12:00 pm	*Buffet Lunch*	Grand Ballroom C
1:00 pm	Resident authored paper and grant awards	
1:10 pm	ACVR Image Interpretation session	
2:40 pm	Presentation on 2011 EAVDI Meeting, Dr. Chris Lamb	
2:50 pm	*Break with Exhibitors*	Grand Ballroom B
3:00 pm	ACVR Business Meeting	
4:30 pm	*Adjourn for the day*	

RO

7:15 am	*Registration opens*	Vanderbilt Registration
9:00 am	**Radiation Oncology Scientific Session 3**	Roosevelt KL
10:00 am	*Break with Exhibitors*	Grand Ballroom B
10:30 am	RO Business Meeting	
12:00 pm	*Buffet Lunch*	Grand Ballroom C
1:00 pm	Resident Authored Paper and Grant Awards	
1:10 pm	ACVR Image Interpretation session	

Thursday, August 19, 2010

7:00 am	Large Animal Diagnostic Imaging Society Meeting	Grand Ballroom A
7:30 am	*Registration opens*	Vanderbilt Registration
8:00 am	CT/MRI Society Keynote Address **Advances in MRI for Microimaging and Cell Tracking** Dr. Paula Foster	
9:00 am	**ACVR Scientific Session 6: CT/MRI**	
10:00 am	*Break with Exhibitors*	Grand Ballroom B
10:30 am	**ACVR Scientific Session 7: CT/MRI**	
12:00 pm	*Buffet Lunch*	Grand Ballroom C
1:00 pm	**ACVR Scientific Session 8: CT/MRI**	
1:30 pm	**ACVR Scientific Session 9:** **Poster Session with Authors**	Grand Ballroom B
2:30 pm	*Break with Exhibitors*	Grand Ballroom B
2:45 pm	Large Animal Diagnostic Imaging Society Keynote Address **Equine Tendon and Ligament Injuries** Dr. Norm Rantanen	
4:45 pm	*Adjourn and Exhibitors close*	

Monday, August 16, 2010

7:00 am	*Registration opens*	Vanderbilt Registration
7:00 am	Veterinary Ultrasound Society Meeting	Grand Ballroom A
8:00 am	**ACVR Forum** **How to Succeed in This Business: A Career Choice Seminar for Radiologists** Introduction: Dr. Jay Stefanacci, 2010 Program Co-Chair	
8:10 am	Radiologists in the Military Dr. Cathy Banfield	
8:38 am	Radiologists in Industry/Corporate America Dr. Bill Hornof	
9:06 am	Radiologists in Academia Dr. Wil Mai	
9:34 am	Radiologists as Sole Proprietors: Mobile Ultrasound, Teleradiography Dr. Sloane Dupree	
10:02 am	*Break with Exhibitors*	Grand Ballroom B
10:12 am	Radiologists as Sole Proprietors: Large Animal (Equine) Dr. Norm Rantanen	
10:40 am	Radiologists as Sole Proprietors: Consultative Services, Teleradiography Dr. Matt Wright	
11:08 am	Discussion and Questions	
12:00 pm	*Buffet Lunch*	Grand Ballroom C
1:00 pm	**Conference Welcome** Dr. Liz Watson, 2010 Program Chair	Grand Ballroom A
1:05 pm	**ACVR Presidential Address** Dr. Marti Larson	
1:35 pm	ACVR Keynote Address **Medical Imaging in the Digital Age: Facing Unexpected Challenges** Dr. Elizabeth A. Krupinski Department of Radiology, University of Arizona	
3:05 pm	*Break with Exhibitors*	Grand Ballroom B

Monday, August 16, 2010

3:30 pm **ACVR Scientific Session 1: General Radiology**
Moderator: Ben Young

3:30 pm **"PAY-PER-VIEW"- A Financial Option for Veterinary Radiologists.**
Robert R. Badertscher II, Consultants in Veterinary Imaging, Naperville, Illinois, 60564.

3:42 pm **Is It Easier to Detect Rib Fractures in a Radiograph Turned On Its Side?**
C.R. Lamb, A.T. Parry, E.A. Baines, Y.M. Chang. The Royal Veterinary College, University of London, Hertfordshire AL9 7TA, U.K.

3:54 pm **Evaluation of Radiographically Apparent Positional Atelectasis in Dogs Breathing 100% Oxygen.**
DY Almondia, J Williams, EH Hofmeister, BA Selcer, S Crochik. University of Georgia, College of Veterinary Medicine, Athens, GA 30602

4:06 pm **Value of Tracheal Bifurcation Angle Measurement as a Radiographic Sign of Left Atrial Enlargement in Dogs.**
A. Le Roux, N. Rademacher, C. Saelinger, D. Rodriguez, R. Pariaut, L. Gaschen Louisiana State University School of Veterinary Medicine, Louisiana, 70803

4:18 pm **Correlation Between "Valentine" Heart Shape, Atrial Enlargement and Cardiomyopathy in Cats.**
R.F. Giglio, M.D. Winter, C.R. Berry, D.J. Reese, H.W. Maisenbacher III University of Florida College of Veterinary Medicine, Gainesville, FL, USA, 32610

4:30 pm *Adjourn for the day*

5:00 pm Opportunity to Meet Resident Coordinators — Grand Ballroom A

6:30 pm *Welcome Reception* — The Vanderbilt Terrace

ACVR KEYNOTE SPEAKER BIOGRAPICAL STATEMENT AND PRESENTATION SUMMARY

Dr. Elizabeth A. Krupinski
Department of Radiology University of Arizona

Radiologists today are being asked to read more and more cases with more and more images per case. This is compounded by shortages in radiologists, especially specialty radiologists in rural and medically underserved areas. The result is that radiologists are working longer hours than ever before. Concerns have been raised regarding fatigue and whether it impacts diagnostic accuracy. The situation for veterinary radiologists is likely quite similar. This talk will review a series of studies designed to determine if radiologists are visually fatigued by their clinical reading, reducing their ability to focus on and accurately interpret images. In one study, forty radiologists viewed 60 skeletal radiographs, half with fractures, before and after a day of clinical reading. Error in visual accommodation (ability to focus) was measured and subjects completed the Swedish Occupational Fatigue Inventory and the oculomotor strain subscale of the Simulator Sickness Questionnaire. Average ROC Az was 0.89 for early and 0.85 for late reading ($F(1,36) = 4.15$, $p = 0.049 < 0.05$). There was greater error in accommodation after a workday ($F(1,14829) = 7.81$, $p = 0.005 < 0.01$), and after the test ($F(1,14829) = 839.33$, $p < 0.0001$). SOFI measures of lack of energy, physical discomfort and sleepiness were higher late in the day ($p < 0.05$). The SSQ measure of oculomotor strain was significantly higher after a day of clinical reading ($F(1,75) = 20.38$, $p < 0.0001$). In a second study, a series of studies that measured eye-position as radiologists scanned images was re-examined to determine if visual search efficiency was impacted as a function of time of day. The data suggest that viewing times are longer later in the day than earlier and the effect seems to be more pronounced for digital images viewed on a computer monitor than for film images viewed on a traditional light box. Dwell times for the individual decisions (TP, FN, FP, TN) also show trends towards longer viewing times in the pm vs am for both film and digital reading. Fatigue may in part be avoided by optimizing the reading room environment so common strategies for optimization will be reviewed.

Dr. Krupinski is a Professor at the University of Arizona in the Departments of Radiology, Psychology and Public Health, and she is Vice Chair of Research in Radiology. She received her undergraduate degree from Cornell University, MA from Montclair State College and PhD from Temple University, all in Experimental Psychology. Her main interests are in medical image perception, assessment of observer performance, medical decision making, and human factors. She is Associate Director of Evaluation for the Arizona Telemedicine Program. She has published extensively in these areas, and has presented at conferences nationally and internationally. She serves on the Editorial Boards of a number of journals in both radiology and telemedicine, and on review panels for NIH, DoD, FDA and TATRC. She is Past Chair of the SPIE Medical Imaging Conference, Past President of the American Telemedicine Association, and Chair of the Society for Imaging Informatics in Medicine.

MEDICAL IMAGING IN THE DIGITAL AGE: FACING UNEXPECTED CHALLENGES

Dr. Elizabeth A. Krupinski
Department of Radiology University of Arizona

The interpretation of medical images relies on a combination of many factors including perception, cognition, human factors, technology, and to some extent innate talent. It is difficult if not impossible to consider any of these in isolation because they interact in a number of both clear and subtle ways. However, when we study the interpretation of medical images, by necessity we sometimes must examine only a single variable at one time in order to try and fully understand its contribution to the overall interpretation process. When one considers how radiologists read medical images, three basic stages are typically regarded as being involved: seeing, recognizing and interpreting. It may sound simple, but the potential for failure at any point in the interpretation process is actually quite high - errors are made. Radiologists need to review the images and see, recognize and interpret the information that is there and render a decision that will affect patient treatment and care. We need to understand not only the images and the technologies used to acquire and display them; we need to understand the interpreter of those images – the radiologist. As the clinical environment changes and more and more various types of images become a part of the patient record this becomes even more critical.

Radiologists today are reading more cases than they did even five years ago, with significantly more images per case. The multiplicity of modalities being used to acquire images during the same course of diagnosis or treatment, as well as the fusion of multi-modal images (e.g., PET-CT) adds to the complexity of the interpretation task and adds significant time as well. The burden is compounded by shortages in radiologists, especially specialty radiologists such as mammographers in rural and medically underserved areas. The result is that radiologists are working longer hours than ever before and some concerns have been raised regarding fatigue and whether it impacts diagnostic accuracy.[1] The situation in veterinary radiology is very similar.[2]

A more recent problem is the reliance on digital imaging. Even the best medical-grade displays available have less contrast than traditional radiographic film and they also have reduced spatial resolution. The problem is that it is that contrast and spatial resolution information is precisely what the visual system uses to regulate image focus, single vision, and direction of gaze. The change to digital displays may have increased strain on radiologists' oculomotor systems, overworking the eyes and resulting in eyestrain (known clinically as asthenopia).[3-5] Close work with digital displays may result in oculomotor fatigue, compounding the effects of longer workdays and aging eyes.[5] A number of studies have confirmed that radiologists can become fatigued after reading cases for a number of hours. Some have demonstrated that there are associated decreases in observer performance (i.e., reduced accuracy).

For example, Gale[6] found a significant morning to afternoon drop in sensitivity in detecting pulmonary nodules in chest radiographs. In a very early study, we polled the radiologists in our department regarding their levels of physical, visual and mental fatigue as a function of number of hours they had been reading and the number of cases they had read. For all measures polled (e.g., blurred vision, double-vision, headaches, back aches, fatigue), we found significant positive correlation between incidence of experienced symptoms and number of cases read and hours reading. The effect was more pronounced when they had been reading digital softcopy as opposed to traditional film. Although intriguing, this study was for the most part subjective and we did not examine diagnostic performance. Encouraged by these results, however, we decided to examine some of our older performance studies to see if we could detect differences in performance between morning and afternoon reading. This retrospective study examined data from four mammography studies[7-10] in which the readers were

required to participate in two test sessions. The records were reviewed to identify which of the subjects completed their test sessions once in the morning and once in the afternoon. Those who completed both in the morning or both in the afternoon were not included in the present analysis. Each study originally had 6 radiologists serving as observers.

Study #1[7] compared screen-film and monitor reading of 20 mammograms (5 mass, 5 microcalcification, 5 mass + microcalcifications, 5 normal) with the lightbox and monitor each at two luminance levels (1100 & 660 ft-L and 140 & 80 ftL respectively). Four of the 6 readers qualified for this analysis (read one condition in the morning and the other in the afternoon) in the screen-film arm and 3 qualified in the monitor arm. Study #2[8] compared mammograms displays on a monitor calibrated to the DICOM Gray Scale Display Function vs calibrated with the SMPTE standard. Three of the 6 readers from this study qualified. Study #3[9] compared CRT vs LCD on and off-axis reading of mammograms and 4 of the six qualified for the present analysis. The fourth study[10] compared digital images that were either processed or not processed with a method to correct for the monitor's MTF and 4 of the 6 readers qualified.

The ROC Az data from the qualifying readers were analyzed with a paired t-test to determine if there were statistically significant differences in diagnostic accuracy as a function of whether the cases were read in the morning vs afternoon. In those studies where eye-position was recorded, these data were examined for potential time of day reading effects as well. It is important to note that for every experiment about half of the trials for each condition were completed in the morning (am) and about half in the afternoon (pm). Therefore, although the experiments were directed at another hypothesis than fatigue effects, the overall differences between am and pm reading cannot be attributed solely to the experimental condition results. On average, the ROC Az for morning (am) performance was 0.924 and was 0.910 for afternoon (pm) reading. The difference was statistically significant ($t = 2.365$, $p = 0.0277$). In general, irrespective of the study they were in and the overall results of those studies, reader performance was lower in the afternoon reading sessions than in the morning reading sessions. Interestingly, the study that compared film and digital viewing revealed no significant differences ($F = 1.445$, $p = 0.2876$) in either modality for am (mean Az film = 0.936, mean Az digital = 0.973) vs pm (mean Az film = 0.938, mean Az digital = 0.970) reading.

In a more recent series of studies, we have hypothesized that the current practice of radiology produces oculomotor fatigue that reduces diagnostic accuracy. Testing this hypothesis first required the ability to measure eyestrain.[11] We develop this capability by measuring visual accommodation of radiologists before and after diagnostic viewing work using an autorefractor that is capable of make multiple measurements of accommodation per second. In the initial study, three radiologists and three residents focused on a simple target placed at near to far distances while accommodation was measured. The target distances varied from 20 cm to 183 cm from the eye. The data were collected prior to and after a day of digital diagnostic viewing.

An Analysis of Variance (ANOVA) was used to examine the data using the accommodation measurements as the dependent variable and target distance, time of day and radiologist vs resident as independent variables. There was a statistically significant difference ($F = 1188.36$, $p < 0.0001$) in the data as a function of target distance, as a function of time of day ($F = 316.10$, $p < 0.0001$), and radiologists vs residents ($F = 271.47$, $p < 0.0001$). Results indicate that accommodation at near distances is significantly worse overall compared to far distances and is significantly worse after a day of digital reading at all distances. Because diagnostic image interpretation is performed at near viewing distances, this inability to maintain focus on the image could impact diagnostic accuracy. As expected, younger residents had better accommodative accuracy than older radiologists.

In a controlled diagnostic accuracy study, Krupinski and Berbaum [12] measured visual accommodation before and after test sessions and had subjects complete the Swedish Occupational Fatigue Inventory (SOFI) [13,14] and the oculomotor strain subscale of the Simulator Sickness Questionnaire (SSQ).[15-17] In one study, forty radiologists at two institutions viewed 60 skeletal radiographs, half with fractures, before and after a day of clinical reading. Average ROC Az was 0.89 for early and 0.85 for late reading ($F(1,36) = 4.15$, $p = 0.049 < 0.05$). There was greater error in accommodation after a workday ($F(1,14829) = 7.81$, $p = 0.005 < 0.01$), and after the test ($F(1,14829) = 839.33$, $p < 0.0001$). SOFI measures of lack of energy, physical discomfort and sleepiness were higher late in the day ($p < 0.05$). The SSQ measure of oculomotor strain was significantly higher after a day of clinical reading ($F(1,75) = 20.38$, $p < 0.0001$). In a second study, a series of studies that measured eye-position as radiologists scanned images was re-examined to determine if visual search efficiency was impacted as a function of time of day. The data suggest that viewing times are longer later in the day than earlier and the effect seems to be more pronounced for digital images viewed on a computer monitor than for film images viewed on a traditional light box. Dwell times for the individual decisions (TP, FN, FP, TN) also show trends towards longer viewing times in the pm vs am for both film and digital reading.

Although most of the image perception, performance and human factors studies have been done with radiologists interpreting images of human anatomy, the essential interpretation process, when viewed as a visual-cognitive activity, differs very little for veterinary radiologists. The key lessons that we have learned over the years by studying the perceptual and cognitive capabilities of radiologists as a function of their working environment can easily be applied to veterinary radiology and there are likely many lessons from veterinary radiology that clinical radiologists would be interested in as well. In the end the goal is the same – more effective and more efficient quality care of patients whether they be animal or human.

REFERENCES:

[1] Krupinski EA, Berbaum KS. Impact of visual fatigue on observer performance. Proc SPIE Med Imag, 2009;7263:72631O-1 – 9.

[2] Poteet, B.A., Veterinary teleradiology. Vet Rad & Ultrasound, 2008;49:S33-S36.

[3] Ebenholtz SM. Oculomotor systems and perception. Cambridge University Press, New York, NY (2001).

[4] MacKenzie W. On asthenopia or weak-sightedness. Edinburgh J Med & Surg, 1843;60:73-103.

[5] Heron G, Charman WN, Gray LS. Accommodation responses and ageing. Investigative Ophthalmology and Visual Science, 1999;40:2872-288.

[6] Gale AG, Murray D, Millar K, Worthington BS. Circadian variation in radiology. In Theoretical and Applied Aspects of Eye Movement Research, AG Gale & F Johnson (eds). Elsevier Science Publishers, London, 1984.

[7] Krupinski, EA, Roehrig, H, Furukawa, T. Influence of film and monitor display luminance on observer performance and visual search. Acad Radiol, 1999;6:411-418.

[8] Krupinski, EA, Roehrig, H. The influence of a perceptually linearized display on observer performance and visual search. Acad Radiol 2000;7:8-13.

[9] Krupinski, EA, Johnson, J, Roehrig, H, Nafziger, J, Lubin, J. On-axis and off-axis viewing of images on CRT displays and LCDs: observer performance and vision model predictions. Acad Radiol 2005;12:957-964.

[10] Krupinski, EA, Johnson, J, Roehrig, H, Engstrom, M, Fan, J, Nafziger, J, Lubin, J, Dallas, WJ. Using a human visual system model to optimize soft-copy mammography display: influence of MTF compensation. Acad Radiol 2003;10:1030-1035.
[11] Krupinski EA, Berbaum KS. Measurement of visual strain in radiologists. *Acad Radiol* 2009;16:947-950.

[12] Krupinski EA, Berbaum. Does reader visual fatigue impact interpretation accuracy. *Proc SPIE Med Imag* 2010; 7627.

[13] Ahsberg, E. Dimensions of fatigue in different workplace populations. Scandinavian J Psych 2000;41:231-241.

[14] Ahsberg, E, Gamberale, F, Gustafsson, K. Perceived fatigue after mental work: an experimental evaluation of a fatigue inventory. Ergonomics 2000;43:252-268.

[15] Kennedy, RS, Lane, NE, Berbaum, KS, Lilienthal, MG. Simulator Sickness Questionnaire: an enhanced method for quantifying simulator sickness. Intl J Aviation Psych 1993;3:203-220.

[16] Kennedy, RS, Lane, NE, Lilienthal, MG, Berbaum, KS, Hettinger, LJ. Profile analysis of simulator sickness symptoms: application to virtual environment systems. Presence 1992; 1:295-301.

[17] Kennedy, RS, Lilienthal, MG, Berbaum, KS, Baltzley, DR, McCauley, ME. Simulator sickness in US Navy flight simulators. Aviation, Space, and Environmental Medicine 1989;60:10-16.

"PAY-PER-VIEW" – A FINANCIAL OPTION FOR VETERINARY RADIOLOGISTS.

Robert R. Badertscher II. Consultants in Veterinary Imaging, Naperville, Illinois, 60564

Introduction/Purpose: In light of the current opportunities for Veterinary Radiologists to generate income, this option provides a reasonable source of full-time income or supplemental income for both well established radiologists, as well as, those starting a private venture. Whether ones primary income stream is from an academic institution, corporate employee, or associated with a specialty center, this offers a unique opportunity for a solo or group of radiologists to increase their monthly revenue.

Methods: This business model establishes the Radiologist as the Owner of DR equip-ment that is remotely located in a satellite private veterinary practice, using the x-ray machine that is already in the facility. The radiologist begins by leasing (5-year) from a vendor (i.e.-Vetel), and places this DR system in the selected clinic in their region. A contract is established between the radiologist and the owner(s) of the private practice to provide exclusive radiographic interpretation service for 100% of the cases imaged. The radiologist maintains ownership of the DR system and provides IT support for the system during the period of the 5-year contract. The teleradiography link from the practice to the radiologist's office is supported through a remote server and viewing software program (i.e.- Asteris) for archival and case reports. A fixed fee per month is charged to the private practice to have the DR system in-house, as well as, a fee per case for radiographic interpretation by the radiologist.

Results: An example for a Pay-Per-View arrangement for a 4 person practice which radiographs at least **50 cases a month** is shown below.

Monthly Expenses for DR System owned by Radiologist and Remotely Installed

Lease Payment on $ 80,000 loan at 8% interest for 5 years	= $ 1,850 / Month
Remote Back-up on Server and Teleradiography Support	= 400 / Month
AVMA Business Insurance on Equipment and Practice	= 200 / Month
Office Equipment & Communications Support	= 200 / Month
TOTAL MONTHLY EXPENSES for 5 –Years	= 2,650 / Month

Monthly Income from DR System – Guaranteed Revenue Stream (100% of Cases)

Fixed Monthly Charge to use DR with 15 Interprets included	= $ 2,550 / Month
Radiographic Interpretation Fee-Additional 35 cases @ $ 50	= 1,750 / Month
TOTAL MONTHLY INCOME for 1st 5-Years	= 4,300 / Month

NET Monthly Income for Initial 5-Years = **$ 1,650 per System ($ 19,800 /Year)**

Discussion/Conclusion: In 2010 there is an addition tax advantage to the Radiologist through the 179 Tax Credit for Equipment Purchase of up to $ 135,000 that results in a $ 28,000 benefit. The projected tax credit for 2011 is slated to drop to only $ 25,000. The ADVANTAGES for this plan is developing a new source of revenue, enhanced case numbers for interpretation, and ownership of equipment. The DETRACTORS include financial risk, set-up and training of staff, failed relationship with practice owners, equipment failure (purchase a 5 year warranty), and management hassles. PITFALLS include over-estimation of caseload, lack of compliance, inferior X-Ray equipment.

IS IT EASIER TO DETECT RIB FRACTURES IN A RADIOGRAPH TURNED ON ITS SIDE? C.R. Lamb, A.T. Parry, E.A. Baines, Y.M. Chang. The Royal Veterinary College, University of London, Hertfordshire AL9 7TA, U.K.

Introduction/Purpose: Radiologists viewing conventional radiographs routinely use various techniques that either increase conspicuity of abnormalities by altering the photographic qualities of the image or increase ability to recognise abnormalities by altering the way the image is perceived. Such techniques may be considered "tricks of the trade" and are widely practised and taught; however, few have been subjected to testing to determine if they really work. The aim of the present study was to test the hypothesis that turning a thoracic radiograph on its side makes it easier to recognise rib fractures.

Methods: Case-control study utilising 120 radiographs of small animal patients all with recent thoracic trauma and either acute rib fractures or no rib fractures, as determined by consensus review of films. Six independent observers representing 3 levels of experience (Radiologist, Resident, Intern) were presented with radiographs at 15 second intervals in a timed PowerPoint presentation. Radiographs were randomised according to species (dog or cat), view (lateral or DV/VD), rib fractures (present or absent), and orientation (conventional or rotated 90 degrees clockwise). For each radiograph, observers stated if rib fractures were visible or not. Associations between outcome (correct diagnosis) and predictor variables were tested using multivariable logistic regressions.

Results: Sixty-five (54%) canine radiographs and 55 (46%) feline radiographs were used. Fifty-nine (49%) radiographs were of animals with rib fractures and 61 (51%) were of animals with no rib fractures. Sensitivity for rib fractures was 57-67% and specificity was 80-95%, depending on the observer. Radiologists had significantly higher accuracy than Residents ($p=0.03$), and Residents had higher accuracy than Interns ($p=0.02$). Compared to less experienced observers, Radiologists had higher specificity ($p=0.0001$) rather than higher sensitivity ($p=0.09$). Overall there was no significant difference in accuracy of diagnosis between dogs and cats ($p=0.36$). Accuracy of diagnosis was significantly reduced when based on lateral radiographs compared to DV/VD views ($p=0.02$) mainly because of low sensitivity of lateral radiographs of dogs. Rotating radiographs 90 degrees clockwise had no effect on accuracy of diagnosis ($p=0.45$).

Discussion/Conclusion: We interpreted "easier" to mean "more likely to be observed within a short time", hence presenting radiographs in a timed PowerPoint presentation was an integral part of the methodology. Although this is unrealistic compared to clinical practice, it was considered necessary because allowing observers unlimited time to view radiographs would have maximized their sensitivity, thus diminishing differences occurring because of the different orientation, and making any effect more difficult to detect; however, even under these conditions, we found no evidence that rotating radiographs 90 degrees clockwise had any effect on accuracy of diagnosis of rib fractures, regardless of the level of experience of the observer. Therefore, this practice cannot be recommended as a diagnostic aid.

EVALUATION OF RADIOGRAPHICALLY APPARENT POSITIONAL ATELECTASIS IN DOGS BREATHING 100% OXYGEN.

DY Almondia, J Williams, EH Hofmeister, BA Selcer, S Crochik. University of Georgia, College of Veterinary Medicine, Athens, GA 30602

Introduction/Purpose: The degree of atelectasis in dependent portions of lung is worsened by the administration of 100% oxygen during general anesthesia, and has been documented in dogs using computed tomography. In our experience, positional atelectasis due to 100% oxygen administration during inhalation anesthesia is commonly seen, and may be misinterpreted as pulmonary disease on routine thoracic radiographs. The purpose of this study was to document the degree of radiographically perceptible positional atelectasis in a 15 minute time period in healthy dogs breathing 100% oxygen via a tightly fitted mask, versus breathing room air.

Methods: Forty healthy client-owned dogs presented to the orthopedic service for elective procedures requiring appendicular/pelvic radiographs under sedation were enrolled. Three view (right and left lateral, and VD) thoracic radiographs were obtained prior to sedation to rule out pre-existing pulmonary disease. Initial lateral recumbency (right or left) and initial treatment (O2 or room air) was randomized. Each dog was sedated and maintained in initial lateral recumbency for 15 minutes breathing O2 or room air; VD and opposite lateral thoracic radiographs were obtained at the end of the 15 minute period. Each dog was then maintained in the opposite lateral recumbency and received the other treatment for 15 minutes. A VD and opposite lateral radiograph was then obtained to complete the study. Post-treatment radiographs were numerically scored for severity of pulmonary pattern and severity of mediastinal shift in the dependent lung by 3 board certified radiologists. The scores were summed for each dog and each treatment to calculate a summary score. A repeated measures ANOVA was used to test for differences in summary, pulmonary, and mediastinal scores between treatments (room air vs. oxygen).

Results: For summary scores, dogs breathing 100% oxygen had significantly higher scores ($p=0.0021$) than dogs breathing room air. Individual scores for pulmonary pattern ($p=0.0155$) and mediastinal shift ($p=0.0032$) were also significantly higher in dogs breathing oxygen vs. room air. Significantly higher summary scores were also seen in right lateral recumbency vs. left, and in dogs with a BCS of 7 vs. 5 (out of 9).

Discussion/Conclusion: Radiographically detectable dependent atelectasis occurs in sedated dogs breathing 100% O2.

VALUE OF TRACHEAL BIFURCATION ANGLE MEASUREMENT AS A RADIOGRAPHIC SIGN OF LEFT ATRIAL ENLARGEMENT IN DOGS.

A. Le Roux, N. Rademacher, C. Saelinger, D. Rodriguez, R. Pariaut, L. Gaschen
Louisiana State University School of Veterinary Medicine, Louisiana, 70803

Introduction/Purpose: Tracheal bifurcation angle on the DV projection has been described in the veterinary literature as a sign of LA enlargement in dogs. The normal angle is currently reported between 60 to 90°.[1,2] In humans, the angle has been shown to be a poor indicator of LA size.[3] The purpose of this study is to evaluate the value of the angle in differentiating normal from increased LA size in dogs.

Methods*:* Thoracic radiographs of 33 normal dogs (ages: 5.0-15.6 years; 3.3-42.1 kg body weight) and 73 dogs diagnosed with MVD (ages: 2.9-16.3; 1.8-49 kg body weight) were reviewed. The LA to aorta ratio (LA/Ao) was determined echocardiographically to classify the LA as normal (LA/Ao≤1.4), mildly (LA/Ao:1.5-1.7), moderately (LA/Ao:1.8-2) or severely (LA/Ao≥2.1) enlarged. An average of three tracheal bifurcation angles was recorded for each dog. Tracheal bifurcation angle and left atrial enlargement was also subjectively assessed by three reviewers. Independent samples *t*-tests were used to compare for differences in the bifurcation angle between normal and abnormal dogs and between severity groups with significance set at $p<0.05$.

Results*:* A significant difference ($p=0.0003$) was observed between the mean angle of 54 dogs with normal LA size (68.1°±8.5,range:51.3-92.4) and that of 52 dogs with enlarged LA (75.8°±8.2,range:57.3-91.7). A significant difference ($p=0.0016$) was also noted between normal dogs and 17 with moderate (75.5°±6.8,range:62.8-88.7) and 19 with severe (80.4°±7.7,range:64.7-91.7)($p<0.0001$) LA enlargement, as well as between 16 dogs with mild (70.7°±7.2,range:57.3-89.9) and severe ($p=0.0006$) LA enlargement. Subjectively, 29 dogs were normal by consensus and had angles of 51.3-72.1. Of these, 24 were normal, 4 had mild and 1 severe LA enlargement. Twenty dogs had increased size and angle and had angles of 72.9-92. Of these, 15 had severe, 4 moderate and 1 normal LA size. An 85.1° angle had a specificity of 92.6% and sensitivity 15.4% for LA enlargement. A 76.6° angle had a specificity of 88.9% and sensitivity of 40.4%.

Discussion/Conclusion*:* Although significant differences in mean angle values were shown between dogs with normal and abnormal LA size, the large degree of overlap in the range of bifurcation angles and its poor sensitivity make the measurement of this angle of little value for diagnosing LA enlargement.

References:

[1] Bahr RJ. Heart and pulmonary vessels. In: Textbook of veterinary diagnostic radiology, 5th Ed. Saunders, 2007: 568-590.
[2] Suter PF, Lord PF. Normal radiographic anatomy and radiographic examination. In: Thoracic radiography: a text atlas of thoracic diseases of the dog and cat. Suter, 1984: 1-46.
[3] Murray JG, Brown AL, Anagnostou EA, et al. Widening of the tracheal bifurcation on chest radiographs: value as a sign of left atrial enlargement. Am J Roentgenol 1995;164:1089-1092.

CORRELATION BETWEEN "VALENTINE" HEART SHAPE, ATRIAL ENLARGEMENT AND CARDIOMYOPATHY IN CATS.

R.F. Giglio, M.D. Winter, C.R. Berry, D.J. Reese, H.W. Maisenbacher III. University of Florida College of Veterinary Medicine, Gainesville, FL, USA, 32610

Introduction/Purpose: On ventrodorsal or dorsoventral radiographs of domestic felines with an enlarged cardiac silhouette, a classic feature often described is the "valentine"-shaped heart (VSH). However, its meaning is somewhat confusing, as some authors correlate this feature to biatrial enlargement, while others to severe left atrial enlargement that displaces the right atrium. The VSH is commonly associated with hypertrophic cardiomyopathy (HCM) by several authors. The purpose of this study is to verify the frequency with which the "valentine" heart shape is associated with biatrial enlargement or left atrial enlargement, and to correlate this feature with the type of cardiomyopathy clinically diagnosed.

Methods: A query of all radiology reports referencing the term "valentine" during the period from January of 2006 to July of 2009 was performed using the RIS database at the University of Florida Veterinary Medical Center. From these results, those patients with thoracic radiography and echocardiography that were performed within a seven days were selected. Upon further review of feline thoracic radiographs by a board-certified radiologist, twelve additional cats that also met the inclusion criteria were considered to have "valentine"-shaped heart. Cardiac chamber enlargement and echocardiographic diagnosis was recorded from the echocardiographic reports. Basic descriptive statistical analysis was performed using a spreadsheet.

Results: A total of 35 cases were included. The results gathered are summarized in the Table 1.

Table 1. Clinical diagnosis and cardiac chamber enlargement, according echocardiographic findings, from cats with "valentine" cardiac shape on thoracic radiographs.

Diagnosis	n	Enlarged chambers						
		RA	RV	LA	LV	LA Only	Biatrial	RA Only
HCM	8	1	0	6	6	5	1	0
RCM	6	4	2	6	3	2	4	0
UCM	10	6	2	8	5	4	6	0
Others	7	3	1	5	2	3	2	1
Normal	3	0	0	0	0	0	0	0
NDD	1	0	0	1	1	1	0	0
Total	35	14	5	26	17	15	13	1

HCM = Hypertrophic cardiomyopathy, RCM = Restrictive cardiomyopathy, UCM = Unclassified cardiomyopathy, Others = Other diagnosis (such as myocardiosis, thyroid toxicosis), Normal = Echocardiographic exam within normal limits, NDD = No definitive diagnosis, Total = Total of cases, n = number of cases, RA, Right atrium, RV, Right ventricle, LA = Left atrium, LV = Left ventricle.

Discussion/Conclusions: The VSH on ventrodorsal or dorsoventral thoracic radiographs of cats is a non-specific finding for HCM or any other type of cardiomyopathy. In cases of HCM, the feature of VSH is likely secondary to severe LA enlargement that displaces the RA. In cases of RCM and UCM, this feature is likely due to biatrial enlargement.

Tuesday, August 17, 2010 ***(ACVR and RO simultaneous sessions)***

ACVR

7:00 am	*Registration opens*	Vanderbilt Registration
7:00 am	**Society of Veterinary Nuclear Medicine Meeting**	Grand Ballroom A
8:00 am	Ultrasound Society Keynote Address **Panel on Ultrasound Contrast** Moderator: Dr. Lorrie Gaschen Panel – Drs. Paul Dayton, Bob O'Brien, Joshua Rychak, Gabi Seiler, and Erik Wisner	
9:30 am	B*reak with Exhibitors*	Grand Ballroom B
9:40 am	**ACVR Scientific Session 2: Ultrasound** Moderator: Gabi Seiler	
9:40 am	**Ultrasound Evaluation of Laryngeal Function in Normal Dogs.** K. Lamoureux, L. Blond, M.C. Blais. Faculty of veterinary medicine, Université de Montréal, P.O. box 5000, St-Hyacinthe (QC), J2S 7C6 Canada.	
9:52 am	**Characterization of Medical Retropharyngeal Lymph Nodes in Clinically Normal Cats Using Ultrasound and Computed Tomography.** S. Nemanic, NC Nelson, JG Hauptman. Michigan State University, Michigan, 48824.	
10:04 am	**Comparing Ultrasonographic Appearances of Nephroliths and Their Artifacts Between Conventional Ultrasound and Spatial Compound Imaging.** Hock Gan Heng, Jacob J Rohleder. Department of Veterinary Clinical Sciences, Purdue University, 625, Harrison Street, West Lafayette, IN 47907.	
10:16 am	**Three Dimensional Ultrasonographic Determination of Renal Volume in the Dog.** N.C. Nelson, A.P. Pease, J.G. Hauptman. Michigan State University, MI 48864.	
10:28 am	**Ultrasonographic Assessment of Long Term Enterectomy Sites in Dogs.** A. Mareschal, D. Penninck, C. RL.Webster. Tufts Cummings School of Veterinary Medicine, North Grafton, MA, 01536.	
10:40 am	*Break with Exhibitors*	Grand Ballroom B

Tuesday, August 17, 2010 ***(ACVR and RO simultaneous sessions)***

ACVR

11:00 am **ACVR Scientific Session 3: Ultrasound**
Moderator: Dr. Lorrie Gaschen

11:00 am **Developing a Technique for Ultrasound-Guided Injection of the Canine Sacroiliac Joint.**
L.M. Gonzalez, J.C. Jones, M.M. Larson, L.E. Freeman.

11:12 am **Combined Ultrasound-Guided Fine Needle Aspiration and Needle Core Biopsy of the Canine Spleen: Report on Safety and Correlation of Test Results.**
A. Watson, D. Penninck, J. Knoll, J. Keating, J. Sutherland-Smith. Tufts Cummings School of Veterinary Medicine, North Grafton, MA, 01536.

11:24 am **The Use of Computed Tomography 3D Reconstructions to Develop Teaching Models for Equine Pelvic Ultrasonography.**
M.B. Whitcomb[1], J. Doval[1], J. Peters[2]. [1]Department of Surgical & Radiological Sciences and [2]William R Pritchard Veterinary Medical Teaching Hospital, University of California, Davis, 95616.

11:36 am **Ultrasonographic Anatomy of Freshwater Stingrays in the Genus Potamotrygon.**
K.B. Wojick[1], K.R. Waller[2], C.P. Poll[3], K.M. Miles[2]. [1]University of Illinois College of Veterinary Medicine, Chicago Zoological and Aquatic Animal Residency Program, Urbana, IL, 61802. [2]Veterinary Clinical Sciences, Lloyd Veterinary Medical Center, Ames, IA, 50011. [3]Department of Animal Health, John G. Shedd Aquarium, Chicago, IL, 60605.

11:48 am **Ultrasonographic Features of Septic Synovial Structures in 62 Horses (2004-09).**
A. Young, M.B. Whitcomb, B. Vaughan, M.H. MacDonald. University of California, Davis, 95616.

12:00 pm *Box Lunch* — The Vanderbilt Terrace

1:00 pm Group trip to the Biltmore — Pickup- Vanderbilt Wing, Level 10

5:00 pm Return

ULTRASOUND EVALUATION OF LARYNGEAL FUNCTION IN NORMAL DOGS.

K. Lamoureux, L. Blond, M.C. Blais. Faculty of veterinary medicine, Université de Montréal, P.O. box 5000, St-Hyacinthe (QC), J2S 7C6 Canada

Introduction/Purpose: Laryngeal paralysis is a fairly common cause of upper airway obstruction in older large breed dogs. Ultrasound allows assessment of paralyzed abduction of the cuneiform processes of the arytenoids cartilage during inspiration and is an alternative to direct laryngoscopy under general anesthesia. However, no objective value is available to detect laryngeal paresis. The goal of this study was to establish normal values of arytenoids cartilage abduction during different breathing pattern using ultrasound in dog.

Methods: Laryngeal ultrasound was performed on 30 large breed dogs (15 less than 6 years of age, 15 older) without respiratory disease. Examination was performed with the dog standing or seated without sedation. Measurement of the maximal arytenoids abduction (MAA) was made during normal inspiration, deep inspiration and painting when possible. Ratios between this distance and the dog's weight and this distance and the left common carotid's diameter (LCCD) during systole were calculated for each inspiration type. Ratios were statistically compared and inference of age or weight was analysed. Significance was set at $p < 0.0001$.

Results: Dogs were of twelve different breeds, 2 were mixed breed. Eighteen dogs were neutered male, 12 were female spayed. Mean weight was 35.12 kg (24.3-78.3 kg). At least one type of inspiration was recorded in all dogs. Only significant difference was identified between the 3 types of inspiration using the ratio MAA/LCCD (values presented in table).

Normal inspiration					
N	Mean	Median	Écart type	Minimum	Maximum
28	0,4832892	0,4664032	0,1268571	0,2727273	0,7555556
Painting					
N	Mean	Median	Écart type	Minimum	Maximum
22	0,9409941	0,9059922	0,2217851	0,6521739	1,6
Deep inspiration					
N	Mean	Median	Écart type	Minimum	Maximum
17	1,2392837	1,326087	0,3377754	0,202	1,6086957

Discussion/Conclusion: Ultrasound allows objective evaluation of normal laryngeal function. Calculation of a MAA/LCCD ratio different from the normal values proposed in this study may help in the detection of laryngeal paresis in large breed dogs with upper airway problem.

CHARACTERIZATION OF MEDIAL RETROPHARYNGEAL LYMPH NODES IN CLINICALLY NORMAL CATS USING ULTRASOUND AND COMPUTED TOMOGRAPHY.

S. Nemanic, N.C. Nelson, J.G. Hauptman. Michigan State University, Michigan, 48824.

Introduction/Purpose: As sites of lymphatic drainage for the nasal and oral cavities, evaluation of the medial retropharyngeal lymph nodes (MRPLN) is important in feline patients with sinonasal disease. The aims of this study were to determine the size of the MRPLN of clinically normal cats using both ultrasound (US) and computed tomography (CT), and to compare measurements made with the two modalities.

Methods: The sample population consisted of 38 adult cats with no prior history of nasal disease. A complete blood count, chemistry panel, FeLV and FIV test and dental charting were obtained, and cats with abnormalities were excluded. All cats were sedated with an intramuscular injection of dexmedetomidine (10 mcg/kg) and butorphanol (0.3 mg/kg). A helical CT examination of the head and neck was performed with 0.625 mm slice thickness and pitch of 0.9375, followed by an ultrasound examination of both MRPLN by two sonographers using a 14MHz linear probe. MRPLN width (W) and height (H) were measured on short axis ultrasound images and transverse CT images at the rostral (Rs), middle (Mid), and caudal (Cd) thirds of the lymph node. Length (L) was measured on long axis ultrasound images and by counting the number of slices spanned by the lymph node on CT. The presence of a hilus and parenchymal homogeneity were evaluated with both modalities. Mean and standard deviation were calculated for each measurement, and US and CT values were compared using multivariate analysis of variance.

Results: Cats were aged 2-8 years, weighed 2.9-8.1kg, and 21 were male and 17 female. The mean measurements and standard deviations (SD) are listed in Table 1. The MRPLN were symmetrical, with no difference between the left and right sides ($p = 0.5$). No measurement exceeded 32mm (L) x 18mm (H) x 8mm (W). The parenchyma was mildly to moderately heterogeneous in all cats.

Table 1	Max L	Rs H	Rs W	Mid H	Mid W	Cd H	Cd W
CT mm (SD)	15.2 (3.9)	13.2 (2.4)	4.7 (0.9)	13.1 (2.3)	4.2 (0.8)	7.7 (2.2)	3.0 (0.8)
US mm (SD)	20.6 (4.1)	12.5 (3.0)	3.8 (0.8)	11.0 (2.5)	3.3 (0.8)	8.8 (2.1)	2.7 (0.8)

Discussion/Conclusion: The normal measurements for feline medial retropharyngeal lymph nodes established here can be used as a baseline for evaluation of clinical patients. Normal MRPLNs are symmetric and have a heterogeneous parenchyma in clinically healthy cats.

COMPARING ULTRASONOGRAPHIC APPEARANCES OF NEPHROLITHS AND THEIR ARTIFACTS BETWEEN CONVENTIONAL ULTRASOUND AND SPATIAL COMPOUND IMAGING.

Hock Gan Heng, Jacob J Rohleder. Department of Veterinary Clinical Sciences, Purdue University, 625, Harrison Street, West Lafayette, IN 47907.

Introduction/Purpose: Spatial compound imaging (SPI) is an important advance in sonographic technology that uses electronic beam steering of a transducer array to rapidly acquire several overlapping scans of an object from different angles. These single-angled acquisitions are averaged to form a multi-angle compound image that is updated in real time. Spatial compound imaging improves image quality by reducing speckle, clutter and other acoustic artifacts such as shadowing and ring-down. The effect of spatial compound imaging on the appearance of the shadowing artifacts caused by nephroliths in small animals is not well-documented. Therefore this study is carried out to document and compare the appearance of nephroliths and shadowing artifacts between conventional ultrasound (CU) and spatial compound imaging.

Methods: Kidneys of small animals with well-visualized radiopaque nephrolith(s) on radiographs were imaged with both conventional ultrasound and spatial compound imaging. The ultrasound system settings were optimized for imaging of a small animal abdomen with a similar depth and focus point location for each set of images. Sets of still images (CU and SPI) showing the nephroliths were captured. The appearances of the nephroliths and shadowing artifacts caused by the nephroliths were evaluated.

Results: A total of 15 kidneys with nephrolith(s) were examined. When using CU, acoustic shadowing artifact was identified in all except for one kidney. Only 7/15 kidneys showed acoustic shadowing artifact when imaged with SPI. The appearance of acoustic shadowing artifact using SPI is different, with multiple weak diverging shadowing artifacts originating from the nephrolith. The far field area of the nephrolith could now be evaluated due to the weaker / disappearing of the shadowing artifacts. The nephroliths now have smooth, better defined margins. They were better visualized due to better contrast of the image quality with SPI. The nephrolith is subjectively bigger and rounded when imaged with SPI.

Discussion/Conclusion: Spatial compound imaging removed or altered the appearance of the acoustic shadowing artifacts caused by the nephroliths. It is thus more difficult to distinguish a nephrolith from other hyperechoic kidney structures such as arcuate vessels. The margins and shape of the nephrolith is better visualized with spatial compound imaging. Therefore, switching between spatial compound imaging and conventional ultrasound is recommended for better evaluation of nephroliths.

THREE DIMENSIONAL ULTRASONOGRAPHIC DETERMINATION OF RENAL VOLUME IN THE DOG.

N.C. Nelson, A.P. Pease, J.G. Hauptman. Michigan State University, MI 48864.

Introduction/Purpose: Assessment of renal volume may be important in cases of renal transplantation or monitoring animals with renal disease. Traditional two dimensional (2D) ultrasound volume assessment relies on measurement of renal length, width, and height and volume calculation based on geometric assumptions of renal shape. A three dimensional (3D) ultrasound method called virtual organ computer-aided analysis (VOCAL) allows rapid volume determination of irregular objects. With this method, an ultrasound volume of an object is acquired. The object is then rotated around its axis, allowing reconstruction of its shape. The purpose of this study is the comparison of 3D and conventional 2D volume determination versus water displacement in assessment of renal volume.

Methods: 19 kidneys from 10 cadaver dogs (weight range 10.3-36.2 kg) were examined ultrasonographically using a GE Logiq 9 ultrasound machine. A microconvex transducer was used to acquire 2D ultrasound images and a microconvex volumetric transducer was used to acquire 3D images. Renal volume was determined using the VOCAL method with a 30 degree rotation angle. Static B-mode images were also acquired of each kidney in dorsal and transverse planes at the level of the renal hilus and maximal length, width, and height were measured of each kidney. Renal volume was calculated using the volume formula for a prolate ellipsoid: length x width x height x 0.524. Kidneys were removed and water displacement volume measurement performed on each kidney. Linear regression was used to assess renal volume by 3D and 2D ultrasound versus water displacement volumes for the left and right kidneys separately and coefficients of determination (R^2) calculated. One way repeated measures analysis of variance was used to compare mean renal volume measurements by each method.

Results: Mean renal volumes determined by 3D and water displacement methods were not significantly different ($p=0.21$). Mean renal volumes determined by 2D and water displacement methods were significantly different ($p<0.01$). 3D and 2D mean renal volumes were also significantly different ($p<0.01$). Coefficients of determination for 3D ultrasound versus water volume measurements were higher than for 2D ultrasound versus water volume measurements. For left kidneys, $R^2 = 0.994$ for 3D ultrasound versus water displacement and $R^2 = 0.944$ for 2D ultrasound volume versus water displacement. For right kidneys, $R^2 = 0.986$ for 3D ultrasound versus water displacement and $R^2 = 0.891$ for 2D ultrasound versus water displacement.

Discussion/Conclusion: 3D ultrasound provides a relatively easy, simple method of renal volume determination with better agreement with water displacement volume measurements than the traditional 2D ultrasound calculation method.

ULTRASONOGRAPHIC ASSESSMENT OF LONG TERM ENTERECTOMY SITES IN DOGS.

A. Mareschal, D. Penninck, C. RL.Webster. Tufts Cummings School of Veterinary Medicine, North Grafton, MA, 01536.

Introduction/Purpose: Immediate post-operative ultrasonographic features of uncomplicated intestinal surgeries have been described[1]. Long-term changes at enterectomy sites are unknown. The purpose of the study is to describe the ultrasonographic features associated with long-term enterectomy sites to establish baseline data facilitating their differentiation from other focal intestinal lesions.

Methods: Twenty-eight enterectomy sites from 28 dogs were sonographically evaluated 6 months post-operatively or later. Documented ultrasonographic features of the enterectomy site included intestinal wall thickness, wall layering integrity, discrete intramural changes, intestinal luminal contents, changes in adjacent tissue, deviation of the anticipated intestinal course, and length of the enterectomy sites.

Results: Enterectomy site visualization was achieved in 78.6% of the dogs. The period of time separating the surgery from the sonographic exam, varied from 7 months to approximately 7 years. A wall thickening was detected in 20/22 dogs (90.9%). The wall layering at the enterectomy site was altered in 20/22 dogs (90.9%) and lost in 2/22 dogs (9.1%). The length of the enterectomy sites ranged from 0.6 cm to 2.5 cm (median: 1.2 cm). Intramural hyperechoic foci were noted in 63.6% of the visible enterectomy sites. A focal accumulation of intraluminal gas was often seen (81.8%) at the enterectomy site. Additional ultrasonographic features included: the presence of an irregular hyperechoic rim bordering the enterectomy site (50%), and a focal deviation of the anticipated intestinal course (45.5%).

Discussion/Conclusion: Most enterectomy sites had persistent wall thickening. None of the visualized enterectomy sites had return to normal layering. The intramural hyperechoic foci most likely representing fibrosis in place of the previous suture material or non-resorbed sutures, can be useful in confirming a former enterectomy site. These descriptive features should assist ultrasonographers in differentiating a previous enterectomy site from other focal intestinal changes.

1. Matthews A, Penninck DG, Webster C. Postoperative ultrasonographic appearance of uncomplicated enterotomy or enterectomy sites in dogs. Vet Radiol Ultrasound 2008;49(5):477-483.

DEVELOPING A TECHNIQUE FOR ULTRASOUND-GUIDED INJECTION OF THE SYNOVIAL COMPONENT OF THE CANINE SACROILIAC JOINT.

L.M. Gonzalez, J.C. Jones, M.M. Larson, L.E. Freeman

Introduction/Purpose: Lower back pain is an important cause of debilitation in large breed dogs, especially those used for working and sporting activities. Early diagnosis and treatment are essential for returning affected dogs to athletic performance. One of the causes of lower back pain in working dogs is sacroiliac osteoarthritis. In humans and horses, ultrasound-guided injection of anti-inflammatory medications into the synovial component of the sacroiliac joint has been described as an effective technique for diagnosing and treating lower back pain due to sacroiliac osteoarthritis. We hypothesized that a similar technique was feasible for use in dogs. The objectives of this study were to 1) describe the normal sectional anatomy of the canine sacroiliac joint and 2) determine optimal sonoanatomic landmarks for guiding needle placement into the synovial component of canine sacroiliac joints.

Methods: Specimens consisting of the caudal lumbar spine, pelvis and hindlimbs were collected from 15 canine cadavers. All dogs had been euthanized at the end of other projects for reasons unrelated to the sacroiliac region. Specimens were positioned in ventral recumbency with the hindlimbs extended caudally and frozen immediately after collection. An oscillating bandsaw was used to slice three of the frozen specimens in transverse, sagittal, and dorsal planes. Digital photographs of both faces of each anatomic slice were acquired and sacroiliac structures were identified and labeled in each photograph. Each of the remaining 12 specimens was thawed for 48 hours, and an 8.5 MHz vector ultrasound transducer was oriented using varying scan planes to guide placement of 22 g 1 ½ inch spinal needles into the synovial components of both sacroiliac joints. In 11 specimens, a mixture of Evan's blue, gelatin, and iodinated contrast medium was injected into the sacroiliac joints. Six of the specimens were dissected immediately following injection to determine the location and distribution of the injected material. Five of the specimens were scanned using computed tomography (CT) immediately after needle placement and injections.

Results: The synovial component is a smoothly marginated, "kidney-bean" shaped structure in the caudoventral portion of the sacroiliac joint. Using a dorsal approach and a transverse ultrasound transducer orientation, optimal sonoanatomic landmarks for accessing this joint space were: the lumbosacral articular process joints, ilial wing, sacral wing, sacral lamina, and median sacral crest. After identifying these landmarks, the sacroiliac joint space could be seen as a triangular, hypoechoic indentation at the junction between the ilial and sacral wings. Using this window, the optimal angle of approach for introducing the needle into the synovial component of the sacroiliac joint was approximately 80 degrees from medial to lateral.

Discussion/Conclusion: Findings indicate that ultrasound-guided injection of the synovial component of the sacroiliac joint is feasible in large breed dogs. Future studies are needed to test the accuracy and intra-operator/inter-operator repeatability of this promising new technique.

COMBINED ULTRASOUND-GUIDED FINE NEEDLE ASPIRATION AND NEEDLE CORE BIOPSY OF THE CANINE SPLEEN: REPORT ON SAFETY AND CORRELATION OF TEST RESULTS.

A. Watson, D. Penninck, J. Knoll, J. Keating, J. Sutherland-Smith. Tufts Cummings School of Veterinary Medicine, North Grafton, MA, 01536

Introduction/Purpose: Percutaneous ultrasound-guided needle core biopsy of the canine spleen is rarely reported. The purpose of this study is to evaluate the safety of percutaneous ultrasound-guided intervention of splenic lesions after fine needle aspiration (FNA) and needle core biopsy (NCB) and to assess the diagnostic value of these two methods.

Methods: Forty-one dogs with sonographically-diagnosed focal or diffuse splenic lesions were prospectively studied. Two or 3 percutaneous FNA and NCB were obtained. Dogs were assessed for post-procedural complications by clinical monitoring and by rechecking a hematocrit with pre-procedure values. Three safety categories were established: no complications, minor complications, and major complications. A clinical and anatomic pathologist independently reviewed each cytology and needle core biopsy sample, respectively, while being blinded to each other's results. Diagnoses were categorized as: neoplasia, benign changes, inflammatory disorder, within normal limits, or non-diagnostic. Cytopathological and histopathological diagnoses were assessed for levels of agreement: complete or partial agreement and disagreement.[1]

Results: Thirty-eight dogs were included in the safety part of the study, and no minor or major complications were encountered. Forty dogs were included in the correlative portion of the study. One dog was excluded due to loss of the FNA sample. Non-diagnostic results from poor sample quality occurred in 1/40 FNA (2.5%) and 5/40 NCB (12.5%). Neoplasia was diagnosed in 17/40 dogs (42.5%), benign changes in 20/40 dogs (50%), inflammatory disorders in 0/40 dogs (0%), and within normal limits in 2/40 dogs (5%). One of the 40 dogs (2.5%) had a diagnosis that was equivocal for neoplasia on both tests and therefore was not categorized. Cytopathological and histopathological diagnoses completely agreed in 16/40 dogs (40%), partially agreed in 3/40 dogs (7.5%), and were in disagreement in 21/40 dogs (52.5%). Of the 17 dogs diagnosed with splenic neoplasia, cytopathological and histopathological results disagreed in 9 dogs. Of these 9 dogs, cytopathology positively diagnosed neoplasia in 6 dogs and histopathology positively diagnosed neoplasia in 3 dogs. In the 8 dogs that were positively diagnosed with neoplasia on both tests, histopathology provided neoplastic subclassification in 6 dogs.

Discussion/Conclusion: Percutaneous FNA and NCB can safely be performed in dogs with sonographic splenic lesions. Preliminary results suggest that adding NCB to FNA provides complementary information in dogs with suspected splenic neoplasia. This combined protocol may improve splenic neoplasia detection and provide neoplastic subclassification.

1. Christensen N, Canfield P, Martin P, Krockenberger M, Spielman D, Bosward K. Cytopathological and histopathological diagnosis of canine splenic disorders. *Aust Vet J*. 2009;**87**: 175-181.

THE USE OF COMPUTED TOMOGRAPHY 3D RECONSTRUCTIONS TO DEVELOP TEACHING MODELS FOR EQUINE PELVIC ULTRASONOGRAPHY.

M.B. Whitcomb[1], J. Doval[1], J. Peters[2]. [1]Department of Surgical & Radiological Sciences and [2]William R Pritchard Veterinary Medical Teaching Hospital, University of California, Davis, 95616.

Introduction/Purpose: Pelvic ultrasonography has gained increased utility in horses with suspect pelvic fractures. Ultrasound is affordable and can be performed on the standing horse in the ambulatory or hospital setting. However, internal pelvic contours can be difficult to appreciate from palpable landmarks, and many find it challenging to translate 3D pelvic contours into a 2D image. Our purpose was to develop 3D simulations of the pelvic ultrasonographic examination for use as instructional aids.

Methods: Contiguous 1mm transverse images were acquired through an equine femur and right hemipelvis using a single slice helical CT scanner[a] from which 3D surface models[b] were created for importation into 3D modeling and animation software.[c] An entire pelvis was next made from a mirror image of the hemipelvis. The 3D femur and pelvic surface models were then positioned into proper anatomic orientation into a 3D horse model.[d] Reference photos were used to create 3D models of large (low frequency) and small (midrange frequency) curvilinear transducers. The ultrasound beam was depicted as a thin sector shape extending from transducer to bone, and the horse's skin was made translucent to permit visualization of pelvic surface contours. The transcutaneous pelvic ultrasonographic examination was created by moving the large curvilinear transducer on the horse's skin surface appropriately to produce images of the ilial wing and body, coxofemoral joint, tuber coxae, tuber ischii and third trochanter of the femur. Transrectal examination was created by placing the small curvilinear transducer "rectally" to examine the ischial body, pubis and axial acetabular surfaces. All animations were exported from the 3D program as QuickTime movie files.

Results: Examination of all ultrasonographically visible pelvic surfaces could be recreated. The full simulation model was readily cropped to generate models of individual pelvic structures. Each model could be rotated to best illustrate the transducer-beam-bone interface. Fractures could be created in any configuration desired, including dynamic fracture simulation. Exported movies were utilized as stand-alone instructional aids or incorporated into presentations or web-based programs.

Discussion/Conclusion: 3D models are uniquely suited for ultrasound instruction by providing a link between technique and image generation. The interaction between the ultrasound transducer/beam and structure of interest can be readily depicted to aid in image interpretation. The addition of the horse's body was important to facilitate understanding of the location and depth of pelvic structures relative to the skin surface. While CT acquisition time was brief, manipulation of images within the 3D software program was time intensive with a steep learning curve. Despite this, results were felt to be worthwhile from an instructional standpoint, and efforts to develop additional novel instructional models are ongoing.

[a]GE Fx/i Helical Scanner, GE, Milwaukee, WS; [b]OsiriX, www.osirix-viewer.com; [c]Cinema 4D, www.maxon.net, Newbury Park, CA; [d]TurboSquid™, www.turbosquid.com, New Orleans, LA

ULTRASONOGRAPHIC ANATOMY OF FRESHWATER STINGRAYS IN THE GENUS *POTAMOTRYGON*.

K.B. Wojick[1], K.R. Waller[2], C.P. Poll[3], K.M. Miles[2]. [1]University of Illinois College of Veterinary Medicine, Chicago Zoological and Aquatic Animal Residency Program, Urbana, IL, 61802. [2]Veterinary Clinical Sciences, Lloyd Veterinary Medical Center, Ames, IA, 50011. [3]Department of Animal Health, John G. Shedd Aquarium, Chicago, IL, 60605.

Introduction/Purpose: Ultrasound is a commonly employed diagnostic tool in aquatic medicine, however, descriptions of normal ultrasonographic anatomy are lacking for most aquatic species. Potamotrygon sp. are freshwater stingrays native to the rivers of South America and are well known for their venomous caudal spine. There are over 15 species of freshwater stingrays in the genus Potamotrygon, with 9 of these species and/or hybrids housed in zoo and aquariums worldwide. Potamotrygon species are also commercially available and may be encountered by veterinarians caring for private fish collections. To aid in the diagnosis of coelomic disease, knowledge of normal ultrasonographic anatomy is essential for evaluation of clinically ill animals. The purpose of this study was to describe the normal ultrasonographic anatomy of the coelomic cavity in healthy freshwater stingrays of the genus *Potamotrygon*.

Methods: Four healthy juvenile wild-caught freshwater stingrays (species *Potamotrygon henlei*), two male and two female, from an aquarium collection were used in the study. Animals were considered to be healthy based on routine physical examination, complete blood count, and continued growth and feeding behavior. Coelomic ultrasound was performed in a water bath with the sedated subject in dorsal recumbency. Organs were identified and B-mode images using a high frequency linear probe were obtained. No coupling gel or standoff pad was used. Ultrasonographic examination lasted 20-30 minutes per animal.

Results: Multiple organs including heart, liver, gallbladder, spleen, esophagus, stomach, small intestine, and spiral colon could be easily identified in all individuals. The liver and spleen are in contact and of similar echogenicity and echotexture. Organs more difficult to delineate included the kidneys, gonads, cloaca, and rectal gland.

Discussion/Conclusion: Ultrasonographic examination of the coelomic cavity of the juvenile freshwater stingray allowed for rapid identification and characterization of a majority of the viscera with minimal stress to the subject. Potential applications include integration with radiography for mechanical obstruction of the gastrointestinal tract, diagnosis of and monitoring of pregnancy, anesthetic monitoring, response to therapy, and serial sonographic screening for detection of subclinical hepatic disease.

ULTRASONOGRAPHIC FEATURES OF SEPTIC SYNOVIAL STRUCTURES IN 62 HORSES (2004-09).

A. Young, M.B. Whitcomb, B. Vaughan, M.H. MacDonald. University of California, Davis, 95616.

Introduction/Purpose: Synovial sepsis is considered a potentially life threatening condition in horses. Route of infection is typically hematogenous in foals. In adults, sepsis is more often due to wounds or iatrogenic causes, including joint injections or surgical procedures. Definitive diagnosis can be challenging, especially when synoviocentesis is complicated by regional lacerations or cellulitis. Radiography +/- contrast fistulography is important in the diagnostic workup, but provides little information regarding soft tissue structures. Ultrasonography has become widely available in equine practice, but ultrasonographic features of synovial sepsis have not been well described.

Methods: Ultrasonographic examinations were reviewed from 62 horses with synovial sepsis confirmed by total nucleated cell count >30,000/ul, neutrophils >90%, bacterial culture and/or evidence of wound communication. Images were reviewed for amount/character of effusion, synovial thickness and estimated synovial thickening-to-effusion (ST:E) ratio.

Results: There were 7 foals, 9 juveniles and 46 adults. Duration of clinical signs prior to presentation was 1-103d with 33% presenting within 48h from onset. Wounds were present in 43 cases. Sepsis involved forelimb (25 horses), hind limb (33) and nonlimb structures (4). Severe lameness (Grade 4-5/5; AAEP lameness grading scale) was present in 84% of horses with limb involvement. Twenty-one separate anatomic structures were affected: digital sheath (18), tibiotarsal joint (7), pastern joint (6), fetlock joint (5), and 4 each: tarsal sheath, calcaneal bursa, lateral femorotibial joint, elbow joint. Other structures were affected in 1-3 cases each. Ultrasound was performed within 48h of presentation to our hospital in 77% (48) horses. Effusions were absent or mild in 63% of affected structures. Synovium was severely thickened in 84% structures, often with an edematous appearance. Forty-nine structures showed >75:25 ST:E ratio and 14 showed 50:50 ratio. Only 4 structures showed severe echogenic effusion. Three horses showed no ultrasonographic evidence of sepsis. Ultrasound identified tendon/ligament injuries in 31 cases and provided guidance for synoviocentesis in 26 affected structures.

Discussion/Conclusion: The predominant feature of severe synovial thickening with or without visible effusion should be considered when evaluating structures for sepsis. Large echogenic effusions were infrequent in our study population. This information should be considered in regions with multiple synovial structures where distention of a specific structure can be obscured by regional swelling. It can also be beneficial when weighing the relative risks and benefits of synoviocentesis, especially in cases with overlying wounds or cellulitis. Finally, ultrasonographic localization of small fluid pockets can assist in the diagnosis of synovial sepsis when combined with ultrasound-guided synoviocentesis, cytological examination and bacterial culture.

Tuesday, August 17, 2010 ***(ACVR and RO simultaneous sessions)***

RO

7:00 am VRTOG meeting — Roosevelt KL

8:00 am Radiation Oncology Keynote Address
Time, Dose, Fractionation
Dr. Colin Orton

9:30 am **Radiation Oncology Scientific Session 1**
Moderator: Dr. Mary Kay Klein

9:30 am **Single Dose 15 Gy Palliative Radiotherapy in 34 Dogs.**
W.M. Adams and E. Kim. University of Wisconsin, Madison, WI, 53706.

9:42 am **DCE-MRI for Detection of Inherent Perfusion Variation in Canine Soft Tissue Sarcomas.**
M.K. Boss[1], N. Muradyan[2], D.Thrall[1]. [1]North Carolina State University, Raleigh, NC, 27606, [2]iCAD, Inc. Nashua NH 03062.

9:54 am **Retrospective Analysis Non-Radiation Complications in Dogs Undergoing Radiation Therapy Treatments.**
Farrelly J[1], Shi Q[2]. [1]Animal Medical Center, New York, NY and [2]New York Medical College School of Health Science and Practice, Valhalla, NY.

10:06 am *Break with Exhibitors* — Grand Ballroom B

10:36 am **Radiation Oncology Scientific Session 2**
Moderator: Dr. Mary Kay Klein

10:36 am **Radiation Therapy for Treatment of Lower Urinary Tract Tumors: A Retrospective of 25 Dogs.**
J Fidel[1], J Lyons[2], J Bryan[1], C Tripp[1], R Sellon[1]
1. Washington State University, Department of Clinical Sciences, Pullman WA, 99163-6610. 2. Veterinary Cancer Group, 9599 Jefferson Blvd., Culver City, CA 90232.

10:48 am **Installation of a Linear Accelerator at the University of Veterinary Medicine Vienna.**
[1]M. Kleiter, [1]C. Schöps, [2]A. Tichy, [1]S. Kosik, [1]M. Willmann, [1]M. Pagitz, [1]B. Wolfesberger. [1]Department for Companion Animals and Horses and [2]Department for Biomedical Sciences, University of Veterinary Medicine Vienna, Vienna, 1210, Austria.

11:00 am **Response Rate and Duration Associated with a 4GY 5 Fraction Palliative Radiation Protocol in Dog and Cats.**
C. McDonald, J.Looper, S.Greene. VCA Aurora Animal Hospital, IL, 60504

Tuesday, August 17, 2010 ***(ACVR and RO simultaneous sessions)***

RO

11:12 am **Total Skin Electron Therapy Technique for the Canine Patient.**
Kerensa N. Rechner[1], Kenneth J. Weeks[2], Amy F. Pruitt[1].
[1]College of Veterinary Medicine, North Carolina State University, Raleigh, NC 27606 and [2] Rex Hospital, Raleigh, NC 27606

11:24 am **Measuring Response of Brain Tumors to Stereotactic Radiosurgery: Interim Results.**
A. L. Zwingenberger, R. E. Pollard, M. S. Kent. University of California, Davis, California 95616.

12:00 pm	*Box Lunch*	The Vanderbilt Terrace
1:00 pm	Group trip to the Biltmore	Pickup- Vanderbilt Wing, Level 10
5:00 pm	Return	

SINGLE DOSE 15 GY PALLIATIVE RADIOTHERAPY IN 34 DOGS.

W.M. Adams and E. Kim. University of Wisconsin, Madison, WI, 53706

Introduction/Purpose: Palliative radiotherapy may provide significant pain relief in dogs with advanced cancer. Various protocols have been reported for dogs, ranging from 1 to 10 fractions of 3 to 10 Gy with total doses of 8 to 32 Gy. Although palliative radiotherapy is a proven method for pain relief, expected short response duration may cause cost / benefit ratio to be a critical factor in treatment decision. Response to a single very high dose of radiation that has been reported for humans was investigated in a series of dogs with large aggressive tumor masses.

Methods: Thirty-four dogs with advanced tumors were given a single 15 Gy dose of cobalt 60 radiation. Treatment was manually planned using a single or bilaterally opposed fields. Treatment field areas ranged from 40 – 500 cm^2; median 75 cm^2. Tumors included lymphosarcoma (11), soft tissue sarcoma (7), osteosarcoma (6), carcinoma (5), melanoma (4) and a mast cell tumor. Ten dogs had known metastasis at time of therapy. Four dogs had previous definitive radiotherapy and 14 had received or were receiving chemotherapy.

Results: Age range was 4 – 13; median 8.5 years and weight range was 6 – 64; median 34 Kg. Tumor volume estimations were available for 23 dogs, ranging from 30 – 2281; median 367 cm^3. Tumor bone invasion was documented in 17 dogs. Clinical response (return to function / pain alleviation) was noted in 24 dogs (71%). No radiation side effects were noted in 32 dogs (94%). One dog had no hair regrowth at the treatment site and 1 dog lost vision in one eye. Survival ranged from 8 – 814 days; median 72 days. Eight dogs lived > 120 days.

Discussion/Conclusion: A single dose of 15 Gy was given to large tumor volumes with minimal side effects. Palliation was attained similar to fractionated palliative protocols reported. Survivals were of short duration in most of these advanced cancer patients, similar to other canine reports using fractionated palliative protocols. Palliative 15 Gy single dose radiotherapy may be a cost-effective alternative in patients with advanced cancer.

DCE-MRI FOR DETECTION OF INHERENT PERFUSION VARIATION IN CANINE SOFT TISSUE SARCOMAS.

M.K. Boss[1], N. Muradyan[2], D.Thrall[1]. [1]North Carolina State University, Raleigh, NC, 27606, [2]iCAD, Inc. Nashua NH 03062

Introduction/Purpose: Assessing tumor perfusion using dynamic contrast-enhanced MRI (DCE-MRI) is a valuable functional endpoint that is linked to tumor phenotype and radiation response. Most DCE-MRI longitudinal therapy response studies rely on one pretreatment assessment of perfusion, but it is not known whether data from one time point reflects native tumor perfusion accurately. Our purpose was to evaluate pre-treatment DCE-MRI for three consecutive days to evaluate the inherent variability in tumor perfusion.

Methods: DCE-MRI studies were performed at 1.5T on three consecutive days prior to any treatment on four dogs with an extremity soft tissue sarcoma. Dogs were under anesthesia for imaging. Prior to contrast medium injection, 3D SPGR T1-weighted images of the entire tumor were acquired at various flip angles and used for quantification of tissue T1 relaxation times. Then, contrast medium was injected rapidly by hand and the entire tumor imaged using the same sequence and a flip angle of 30°. Contrast medium was injected 1 minute into the dynamic series, which consisted of 80 acquisitions of approximately 8sec each. Perfusion parameters were quantified and extracted in the 6 central slices of the tumor on each day using CADvue®, employing a Toft's-based 2-compartment model to estimate the transfer constant K^{trans}, v_e - the extravascular extracellular volume fraction, and the rate constant k_{ep}.

Results: In two dogs the tumor perfusion parameters were relatively stable over the three study days. In two other dogs, however, variation was observed in K^{trans} and k_{ep} while the v_e remained relatively stable. This variation was characterized by increased K^{trans} and k_{ep} on day 2 compared to days 1 and 3. The AIF and reference muscle tissue had similar parameters for all 3 days.

Discussion/Conclusion: Our data suggest there may be inherent daily variations in tumor perfusion parameters in some tumors. We did not identify technical issues such as differences in positioning that would account for this variation. Acute changes in tumor oxygenation due to changes in tumor perfusion, i.e. acute hypoxia, have been recognized for years. However, that acute hypoxia is associated with large regional perfusion changes has not been elucidated. Our data suggest that obtaining a single pretreatment estimation of tumor perfusion using DCE-MRI may not be adequate in longitudinal studies where baseline data will be compared to subsequent post-treatment determinations.

Supported in part by NCI grant CA29582

RETROSPECTIVE ANALYSIS OF NON-RADIATION COMPLICATIONS IN DOGS UNDERGOING RADIATION THERAPY TREATMENTS.

Farrelly J[1], Shi Q[2]. [1]Animal Medical Center, New York, NY and [2]New York Medical College School of Health Science and Practice, Valhalla, NY.

Introduction/Purpose: Dogs undergoing radiation therapy can develop complications from anesthesia or hospitalization that accompanies treatment. To the author's knowledge no study to date has described complications in clinical patients undergoing multiple episodes of anesthesia for radiation therapy treatments. The purpose of this retrospective study was to characterize the incidence and type of complications that occur in dogs undergoing radiation therapy.

Methods: Medical records of all dogs treated with radiation at the Animal Medical Center between September 2004 and June 2007 were reviewed. All dogs receiving at least one treatment were included in the study. Demographic and clinical characteristics such as age, breed, gender, body weight, tumor type, tumor location, number of treatments, abnormalities on pre-treatment blood work, and whether or not chemotherapy, glucocorticoids or nonsteroidal anti-inflammatory drugs were given were collected. The number of non-radiation complications and their type and severity were recorded. Complications that could be attributed to the tumor or the effects of radiation were excluded. Statistical analyses were performed to determine whether those demographic and clinical characteristics were associated with development of a complication.

Results: A total of 267 dogs were included and this represented 272 courses of radiation with 2334 individual treatments. General anesthesia was used for all treatments. Complications occurred in 101 (37%) dogs. Common side effects included cough, vomiting and diarrhea which were typically self limiting. In 17 cases (6%) the complication resulted in a treatment delay or hospitalization. In 8 dogs (3%) the complication resulted in either euthanasia or death. Dogs that developed complications were younger, received more treatments, had elevated white cell count, received glucocorticoids during treatment, but were less likely to have thrombocytopenia. On multivariate analysis only elevated white cell count was significant.

Discussion/Conclusion: Findings from this study indicate that complications, other than those caused by radiation, are common in dogs undergoing anesthesia for multiple radiation treatments. However, these complications are usually mild or self limiting.

RADIATION THERAPY FOR TREATMENT OF LOWER URINARY TRACT TUMORS: A RETROSPECTIVE OF 25 DOGS.

J Fidel[1], J Lyons[2], J Bryan[1], C Tripp[1], R Sellon[1]
1. Washington State University, Department of Clinical Sciences, Pullman WA, 99163-6610.
2. Veterinary Cancer Group, 9599 Jefferson Blvd., Culver City, CA 90232

Introduction/Purpose: For treatment of tumors the lower urinary system in dogs radical surgery is often not compatible with quality of life and with chemotherapy alone median survivals are still less than 1 year. If dogs are obstructed other measures such as placement of cystostomy tubes are often necessary. Human lower urinary tract tumors are treated with radiation therapy particularly for prostate but also for bladder when complete cystectomy is thought to be inappropriate. Radiation of canine lower urinary tract tumors has not been routinely performed and severe side effects have been reported with coarse fractionation schemes. The purpose of this study was to retrospectively evaluate cases of bladder and prostate radiation from Washington State University and the Veterinary Cancer Group in the past 5 years and note what role radiation played for extension of life and increase in life quality for these patients.

Methods: Tumors of prostate or bladder were diagnosed via biopsy of cytology. Dogs were treated with a variety of fractionation schemes summarized as palliative intent- 20- 27 Gy in 2.5- 5 Gy fractions; or curative intent with 45- 54 Gy in 2.5 or 2.7 Gy fractions. All dogs were treated with parallel opposed beams and overall treatment time varied from 5- 24 days.

Results: Eighteen dogs were treated with doses ≤27 Gy, and 7 were treated with doses of 45-54 Gy, with no significant difference in survival between these two groups. Urinary obstruction was found in 17 dogs and 16 dogs were able to urinate on their own at a median of 7 days after starting therapy. Median survival for all dogs was 124 days with bladder (n=12) surviving longer than prostate (n=13); median survival of 195 days versus 47 days, P= 0.0443. Cause of death was metastasis in 11 dogs (9/11 of prostate) with median survival of 41 days, and local disease in 10 dogs with median survival 143 days; this was significantly different (P=0.0040). Whether the dogs received any treatment prior to RT, received chemotherapy with RT or after, or received piroxicam versus other NSAID's did not effect survival. Signs of colitis was seen in 8/25 dogs in the acute period but no late effects were seen in any of the dogs.

Discussion/Conclusion: Radiation of bladder and prostate tumors can help relieve urinary tract obstruction quickly and safely. Use of a palliative protocol may be equally effective and with prostate tumors may be ideal due to the high rate of metastasis early in the course of the disease.

INSTALLATION OF A LINEAR ACCELERATOR AT THE UNIVERSITY OF VETERINARY MEDICINE VIENNA.

[1]M. Kleiter, [1]C. Schöps, [2]A. Tichy, [1]S. Kosik, [1]M. Willmann, [1]M. Pagitz, [1]B. Wolfesberger. [1]Department for Companion Animals and Horses and [2]Department for Biomedical Sciences, University of Veterinary Medicine Vienna, Vienna, 1210, Austria.

Introduction/Purpose: Radiation Oncology has become an important treatment modality in the battle against cancer in dogs and cats. In Europe the implementation of radiotherapy units into veterinary institutions took longer than in the USA but is currently a fast developing process. At the University of Veterinary Medicine Vienna a linear accelerator was installed in 2005 and radiotherapy treatments started in January 2006. The aim of this study was to analyze the first patient cohert treated at this institution retrospectively.

Methods: Dogs and cats with cancer which received radiation therapy in the years 2006-2008 were included into this study. Medical records of patients were reviewed and national, tumor type, tumor location, radiotherapy treatment protocols and adjuvant treatment modalities were recorded. Follow-up informations were obtained from the medical records and by phone conversations with referring veterinarians and pet owners.

Results: A total of 255 patients were irradiated in the three year time period. The majority of these patients came from Austria (n=166), followed by patients from Italy (n=42). The remaining animals were referred from eight European countries and from Israel. Dogs (n=178) were more frequently treated than cats (n=77). Head and neck tumors were the most common cause for radiotherapy (52%), followed by tumors on the trunc (27%) and the extremities (21%). Surgery was performed prior radiotherapy in 128 patients with 63 of them presenting with recurrent disease. In 28 patients the tumor was resected after radiotherapy. Chemotherapy was given in 117 animals. Definitive radiotherapy was prescribed in 143 patients and coarse-fractionated or palliative radiotherapy in 112 animals. In the latter group the median survival time was 187 days and in the definitvely irradiated group it was 578 days.

Discussion/Conclusion: Radiotherapy was generally accepted as new treatement modality by pet owners and referring veterinarians. However, 44% of all patients received only coarse-fractionated or palliative radiotherapy. Underlying causes might be remaining skepticism towards more aggressive treatment protocols and repeated anesthesia, high costs for definitive radiotherapy and referral of cases with advanced disease. The high number of irradiated head and neck tumors reflects the challenge of wide resections in this location, and the high number of patients receiving combination therapies shows an increasing use of multimodality treatment regiments in small animal oncology.

RESPONSE RATE AND DURATION ASSOCIATED WITH A 4GY 5 FRACTION PALLIATIVE RADIATION PROTOCOL IN DOGS AND CATS.

C. McDonald, J.Looper, S.Greene. VCA Aurora Animal Hospital, IL, 60504

Introduction/Purpose: Palliative radiation therapy is an important treatment option for our veterinary cancer patients. The goal is to maintain or improve quality of life by providing improvement in clinical signs while minimizing toxicity. This protocol provides a conservative dose using a relatively small fraction size and short overall treatment duration. The purpose of this study was to determine whether 4Gy fractions over 5 consecutive days is an effective and safe palliative radiation protocol for dogs and cats.

Methods: Retrospective analysis was performed to identify patients with complete follow up that completed the 5 fractions of 4Gy given on consecutive days for a total of 20Gy. Signalment, dates of treatment, response to treatment, duration of response, cause of death, and date of death were determined from medical records, referring veterinarian or verbal communication. Type of treatment and adjunctive therapy were also reported.

Results: One hundred fifty five patients were treated with this protocol between June 30, 2005 and October 25, 2009. Seventy-four patients (19 cats, 55 dogs) had complete follow up information and were included in this study. Overall response rate (ORR) for all patients was 71.6%. Median duration of response (MDOR) was 2.9 months and median survival time (MST) was 4.4 months. Primary bone tumors were the most common tumors treated. Sites included humerus, rib, vertebra, mandible, maxilla. Four fibrosarcomas(2 cats), 4 osteosarcomas, 3 multilobular tumors of bone, and 6 unknown types of sarcomas were treated. The ORR for primary bone tumors was 76.4%. MDOR was 2.9 months and MST was 3.5 months. The most common tumor treated in cats was squamous cell carcinoma and ORR was 66.6%. MDOR was 2.6 months and MST was 3.0 months. With exception of primary bone tumors, soft tissue sarcomas were the next most common tumor treated in dogs(10). ORR was 80% and the 2 other patients had stable disease. MDOR was 5.9 months and MST was 7.5 months. Seven cases of apocrine gland anal sac adenocarcinoma were also treated. ORR was 71.4%. MDOR was 8 months and MST was 7.3 months. Other commonly treated tumors in dogs were 5 nasal carcinomas, 5 prostatic tumors (4 carcinomas and 1 osteosarcoma), and 3 subcutaneous hemangiosarcomas. Overall rate of toxicity was 18.8% in 64 patients that were evaluated for toxicity. Ten patients had acute and 3 had late. All but 2 incidences of acute toxicity were grade I. Onset of acute toxicity ranged from 2 to 3 weeks following completion of the protocol. All incidences of late toxicity were grade I alopecia and leukotrichia.

Discussion/Conclusion: Five consecutive daily fractions of 4Gy appear to be sufficient to palliate veterinary patients with a variety of tumors. Toxicities when reported were very mild and did not significantly impair quality of life. Future directions include direct comparison with traditional 8Gy 4 fraction palliative protocols to compare response rates and duration.

TOTAL SKIN ELECTRON THERAPY TECHNIQUE FOR THE CANINE PATIENT.

Kerensa N. Rechner[1], Kenneth J. Weeks[2], Amy F. Pruitt[1].
[1]College of Veterinary Medicine, North Carolina State University, Raleigh, NC 27606 and [2] Rex Hospital, Raleigh, NC 27606

Introduction/Purpose: Cutaneous Epitheliotropic T Cell Lymphoma (mycosis fungoides) in canine patients is a rare condition with many similarities to the human form of the disease and a moderately poor response to conventional chemotherapy. In humans, radiation therapy is the most effective single agent for the treatment of this disease. With the development of electron beam therapy, patients have been effectively treated with total skin electron therapy. In vitro, canine cutaneous T-cell lymphoma cells have been shown to be radiation sensitive; however, canine total skin electron therapy has been rarely used in clinical practice. The purpose of this study was to evaluate dose distribution with a technique for total skin electron therapy using 6 MeV electron beams and 6 dual-fields**.**

Methods: Treatment set up involved two positions for a canine patient in lateral recumbency under general anesthesia. The first position created two vertical dual fields with the patient on the floor under the gantry 231.5 cm from the source. The gantry was rotated ±25 degrees from the vertical axis to create cranial and caudal fields. The second position created four oblique junction fields with the patient on the floor and across the room. The gantry is rotated 60 degrees away from vertical with the treatment field projected at 230 cm from the vertical axis of the gantry. The patient is moved along the central axis of the beam to cover oblique cranial and caudal portions for both the ventral and dorsal aspects of the body. Each position is repeated to treat right and left aspects of the body. Uniformity, flatness and symmetry of the radial and transverse planes were determined for all fields. Dosimetry was calculated according to the TG-21 protocol using ionization chambers for both positions to determine cGy per MU at a depth of 5 mm. The combined result of all beams was measured to create a percent depth dose profile for total body skin dose. “In vivo” skin dose was measured on a canine cadaver with thermoluminescent dosimeters.

Results: The dimensions of both positions were adequate to obtain an effective treatment profile for the entire thickness of a canine patient’s epidermis. There was a ±3.0% and 0.5% skin dose variation between the transverse fields and sagittal fields respectively comparing the vertical and oblique junction fields. The thermoluminescent dosimeters indicated a dose variation over the cadaver skin of ± 6.8%.

Discussion/Conclusion: The extremities proved to have the most uneven dose distribution, suggesting that shielding these areas and using separate treatment fields will be necessary during patient treatment. This technique for total skin electron therapy in canine patients was technically feasible and provided a dose distribution similar to accepted human standards of treatment.

MEASURING RESPONSE OF BRAIN TUMORS TO STEREOTACTIC RADIOSURGERY: INTERIM RESULTS.

A. L. Zwingenberger, R. E. Pollard, M. S. Kent. University of California, Davis, California 95616.

Introduction/Purpose: Stereotactic radiosurgery (SRS) is a single fraction highly conformal high-dose radiation therapy technique used to treat cancer. This study was designed to evaluate the response to SRS treated tumors using size and perfusion parameters.

Methods: Dogs and cats with intracranial tumors involving the brain, pituitary and cranial nerves were enrolled. Animals were treated with either 15Gy in one fraction or 24Gy in 3 fractions using individually designed and tested radiation treatment plans. All treatment plans were done using computerized treatment planning software. Pre-treatment imaging included a CT scan and an MRI scan, except for pituitary tumors in which only a CT scan was done. The CT scan included a dynamic acquisition over 90 seconds with non-ionic iodinated contrast given at a rate of 5 mL/s intravenously. Post-treatment imaging was performed at 3 months, and included dynamic CT and brain MRI scans.

Results: To date 11 patients have been treated and three have been re-imaged. Perfusion maps were generated at both time points and regions of interest placed in the tumor, brain, and peripheral tissues. Dimensions and volume of tumor were calculated. The changes in size and perfusion of tumor imaged to date will be presented.

Discussion/Conclusion: Changes in tumor size and volume may be used to monitor response to SRS therapy in brain tumors.

Wednesday, August 18, 2010 ***(ACVR and RO simultaneous sessions)***

ACVR

7:15 am	*Registration opens*	Vanderbilt Registration
7:15 am	CT/MRI Society Meeting	Grand Ballroom A
8:15 am	Nuclear Medicine Society Keynote Address **Molecular Imaging: Technology, Tracers and Translation** Dr. Jon Wall	
9:45 am	*Break with Exhibitors*	Grand Ballroom B
10:00 am	**ACVR Scientific Session 4: Nuclear Medicine** Moderator: Federica Morandi	
10:00 am	**Targeted Imaging of the alpha4-beta1 integrin in Canine Lymphoma.** A. L. Zwingenberger, M. S. Kent, R. Liu, K. S. Lam, E. R. Wisner University of California, Davis, California, 95616.	
10:12 am	**Maximum Standard Uptake Values of 18FDG in Confirmed Canine Primary Malignant Tumors and Their Metastasis.** D.S. Gibbons[1], S. Ryan[2], S. Lana[2], S. LaRue[1], S.L. Kraft[1]. Department of Environmental and Radiological Health Sciences[1] and Animal Cancer Center[2], Colorado State University, Fort Collins, CO 80523.	
10:24 am	**Serial 18FDG-PET/CT can Assess Response to Receptor Tyrosine Kinase Inhibition in Canine Cancer.** A.K. LeBlanc[1,2], F. Morandi[1], A.N. Miller[1], J.S. Wall[2], G.D. Galyon[1], T.D. Moyers[1], M.J. Long[2], A.C. Stuckey[2]. University of Tennessee, [1]College of Veterinary Medicine, [2]Graduate School of Medicine, Molecular Imaging and Translational Research Program; Knoxville, TN, 37996.	
10:36 am	**Renal Scintigraphy in Nine Bottlenose Dolphins Using Technetium-99m Mercaptoacetyltriglcine (^{99m}TC-MAG3).** C.R. Smith[1], M. Solano[2], S.P. Johnson[1], S.K. Venn-Watson[1], E.D. Jensen[3], C.K. Hoh[4]. [1]National Marine Mammal Foundation, CA 92106; [2]Tufts University, Cummings School of Veterinary Medicine, MA 01604; [3]Navy Marine Mammal Program, SSC PACIFIC, CA 92152; [4]University of California San Diego Medical Center, CA 92103.	
10:48 am	*Break with Exhibitors*	Grand Ballroom B
11:12 am	**ACVR Scientific Session 5: Nuclear Medicine & General Radiology** Moderator: Jay Stefanacci	
11:12 am	**Technetium 99m Thyroid to Background (T:B) Ratios for Feline ^{131}I Treatment Successes and Failures Using 4 mCi I-131.** S.T. Wallack[1], M. Metcalf[1], A. Skidmore[1], C. Lamb[2]. Veterinary Imaging Center of San Diego, CA, 92111[1]. The Royal Veterinary College, UK, AL9 7TA[2].	

Wednesday, August 18, 2010 ***(ACVR and RO simultaneous sessions)***

ACVR

11:24 am **Feline ^{131}I Treatment Successes and Failures Using a Dual Dosing Protocol of 4 mCi or 7 mCi I-131 Based on the T:B Ratio.**
S.T. Wallack[1], A. Bettencourt[1], J. Balairon[1], C. Lamb[2]. Veterinary Imaging Center of San Diego, CA, 92111[1]. The Royal Veterinary College, UK, AL9 7TA[2].

11:36 am **Optimization of Small Animal Digital Radiographic Technique to Maximize Signal to Noise and Evaluate the Effects on Personnel Exposure.**
C.N. Copple, I. D. Robertson,
and D. E. Thrall. North Carolina State University, North Carolina, 27606

11:48 am **Training Residents to Write Meaningful Reports.**
P.V. Scrivani, N.L. Dykes, M.S. Thompson, A.E. Yeager. Cornell University, NY 18453.

12:00 pm *Buffet Lunch* Grand Ballroom C

1:00 pm Resident Authored Paper and Grant Awards

1:10 pm ACVR Image Interpretation Session

2:40 pm Presentation on European Assoc. of Veterinary Diagnostic Imaging (EAVDI) 2011 Meeting, Dr. Chris Lamb

2:50 pm *Break with Exhibitors* Grand Ballroom B

3:00 pm ACVR Business Meeting

4:30 pm *Adjourn for the day*

TARGETED IMAGING OF THE ALPHA4-BETA1 INTEGRIN IN CANINE LYMPHOMA.

A. L. Zwingenberger, M. S. Kent, R. Liu, K. S. Lam, E. R. Wisner University of California, Davis, California, 95616

Introduction/Purpose: Activated alpha4-beta1 integrin has increased expression on the cell membrane of lymphoma cells. A peptidomimetic compound (LLP2A) was developed using the one-bead-one-compound (OBOC) screening method to target this integrin. This study was designed to characterize the affinity of LLP2A to canine lymphoma cells in vitro and in vivo.

Methods: Flow cytometry was used to test the affinity of LLP2A to fine needle aspirates from lymph nodes of dogs with lymphoma. A candidate agent for planar scintigraphy was synthesized as both PEGylated and unPEGylated formulations (^{99m}Tc-Hynic-LLP2A, ^{99m}Tc-Hynic-LLP2A-PEG). The radiotracers were used to image 3 normal dogs and 5 dogs with lymphoma. The biodistribution to tumor, major organs and clearance from the blood were measured.

Results: Flow cytometry revealed good affinity for canine lymphoma cells as compared to normal lymphoid cells. Normal canine imaging revealed significant differences in biodistribution of the PEGYlated and unPEGylated LLP2A formulations. Imaging of lymphoma dogs revealed increased uptake in affected lymphoid tissue with regions of increased activity correlating well with findings from other cancer staging imaging modalities.

Discussion/Conclusion: This study confirms affinity of LLP2A to canine lymphoma cells in vitro using flow cytometry, and in vivo using ^{99m}Tc-Hynic-LLP2A and ^{99m}Tc-Hynic-LLP2A-PEG. The chemical properties of LLP2A offer the possibility of developing multiple targeted imaging and therapeutic agents.

MAXIMUM STANDARD UPTAKE VALUES OF ^{18}FDG IN CONFIRMED CANINE PRIMARY MALIGNANT TUMORS AND THEIR METASTASES.

D.S. Gibbons[1], S. Ryan[2], S. Lana[2], S. LaRue[1], S.L. Kraft[1]. Department of Environmental and Radiological Health Sciences[1] and Animal Cancer Center[2], Colorado State University, Fort Collins, CO 80523.

Introduction/Purpose: The maximum standard uptake value (mSUV) is the most clinically utilized parameter of ^{18}FDG accumulation in tissues, allowing for a semi-quantitative estimation of the rate of glycolysis based on radiopharmaceutical metabolism[1].The pattern of ^{18}FDG uptake and standard uptake values have been described in the normal dog[1] and cat[2], and the pattern of ^{18}FDG uptake was described in dogs diagnosed with lymphoma and mast cell tumors[3]. This report presents the mSUVs of confirmed canine primary malignant tumors and/or their metastases.

Methods: ^{18}FDG-PET/CT imaging was performed on eight dogs diagnosed with a primary malignant tumor, and one dog for metastasis of a known primary malignant tumor. One dog underwent a second ^{18}FDG-PET/CT procedure following stereotactic body radiation therapy of a primary bone tumor. Whole body CT and PET imaging was performed using a standard protocol, with PET images acquired 60 minutes following ^{18}FDG administration for all dogs. Tumor volume and mSUVs were derived from commercial software (Extended Brilliance Workstation, Phillips Medical Systems).

Results: Five breeds were represented. Ages ranged from 6.83 to 12.92 years, (mean 9.75 yr). Nine primary tumor types were identified in eight dogs. Metastasis was identified in two of these eight dogs and in the dog imaged specifically to determine the extent of metastatic disease secondary to left humeral osteosarcoma. Ten metastatic lesions (regional lymph nodes, lung, liver and pleura/mediastinum) were identified. Primary tumor volumes ranged from 1.5-160.6 cm^3, with a mean of 64.6 cm^3. Maximum SUVs of the primary tumors ranged from 3.4-25.9, with a mean of 10.6 (n=9). Maximum SUVs for metastatic lesions ranged from 1.9-7.8, with a mean of 4.2 (n=10) and mean volume of 39.80 cm^3 (range 0.48-254.86 cm^3). The mSUV of the primary bone tumor following stereotactic radiotherapy decreased to 1.7 from a pre-therapy value of 7.8.

Discussion/Conclusion: A wide range of tumor volumes and mSUVs were detected for canine primary and metastatic neoplasms. Primary tumor mSUV was not related to its tumor volume (R^2=0.0983). However, the lower mSUVs of metastatic lesions may relate, at least in part, to some of the lesion volumes being small relative to PET spatial resolution. Maximal SUVs have prognostic value for many human malignancies[1] but a similar utility of canine mSUVs has not yet been determined as this technology is new to veterinary medicine. Maximal SUVs are influenced by numerous factors including tumor volume, histology, anatomic location, plus equipment and protocol factors[1].

1. LeBlanc, AK, et al. Vet Rad & Ultrasound 2008; 49(2):182-188.
2. LeBlanc, AK, et al. Vet Rad & Ultrasound 2009; 50(4):436-441.
3. LeBlanc, AK, et al. Vet Rad & Ultrasound 2009; 50(2):215-233.

SERIAL ^{18}FDG-PET/CT CAN ASSESS RESPONSE TO RECEPTOR TYROSINE KINASE INHIBITION IN CANINE CANCER.

A.K. LeBlanc[1,2], F. Morandi[1], A.N. Miller[1], J.S. Wall[2], G.D. Galyon[1], T.D. Moyers[1], M.J. Long[2], A.C. Stuckey[2]. University of Tennessee, [1]College of Veterinary Medicine, [2]Graduate School of Medicine, Molecular Imaging and Translational Research Program; Knoxville, TN, 37996.

Introduction/Purpose: Palladia™ (toceranib phosphate – Pfizer Animal Health) is a novel orally-administered receptor tyrosine kinase (RTK) inhibitor recently approved for treatment of canine mast cell disease. Receptor tyrosine kinases are important mediators in several cellular processes and when dysregulated lead to tumor growth, progression, and metastasis. Palladia™ has been shown to target vascular endothelial growth factor receptor (VEGFR-2/Flk-1/KDR), platelet derived growth factor receptor, and Kit. Positron Emission Tomography/Computed Tomography (PET/CT) is commonly used to diagnose, prognosticate, and monitor response to anti-neoplastic therapy in cancer patients. In this study, serial PET/CT imaging with ^{18}F-fluorodeoxyglucose (^{18}FDG) was used to assess response to Palladia™ therapy in dogs with measureable solid malignancies.

Methods: Seven dogs with various solid malignancies underwent whole body contrast-enhanced PET/CT with ^{18}FDG (4.547±0.77 mCi, mean ±SD) after 60 minute uptake time using a 64-slice PET/CT scanner (Siemens mCT, Siemens Molecular Imaging, Knoxville, TN). Six dogs were imaged at the time of diagnosis (baseline); one dog underwent CT only at baseline. All dogs underwent PET/CT and at a median of 5.5 weeks post-baseline (first recheck; range: 4-10 weeks). Two dogs underwent additional PET/CT scans at 14 weeks, and at 10 and 15 weeks post-baseline respectively. Images were correlated to treatment response. Drug-related toxicities were recorded.

Results: One dog demonstrated significant clinical improvement at the first recheck and was maintained on the drug despite dose modification due to toxicity; measureable clinical and image-based response was seen after 12 weeks of therapy. All other dogs demonstrated stable or progressive disease based on follow-up clinical staging and PET/CT at the first recheck. Scan results agreed with clinical assessment of externally measurable disease. Palladia™ therapy was continued in patients with stable disease and acceptable drug tolerance, and was discontinued in non-responsive patients.

Discussion/Conclusion: PET/CT with ^{18}FDG can be used to monitor clinical response to Palladia™. Further studies are needed to better assess the clinical usefulness of Palladia™ in tumor-bearing dogs.

RENAL SCINTIGRAPHY IN NINE BOTTLENOSE DOLPHINS USING TECHNETIUM-99m MERCAPTOACETYLTRIGLYCINE (^{99m}TC-MAG3).

C.R. Smith[1], M. Solano[2], S.P. Johnson[1], S.K. Venn-Watson[1], E.D. Jensen[3], C.K. Hoh[4]. [1]National Marine Mammal Foundation, CA 92106; [2]Tufts University, Cummings School of Veterinary Medicine, MA 01604; [3]Navy Marine Mammal Program, SSC PACIFIC, CA 92152; [4]University of California San Diego Medical Center, CA 92103.

Introduction/Purpose: Ammonium acid urate nephrolithiasis has been reported as a clinically significant disease in managed populations of bottlenose dolphins (*Tursiops truncatus*). The impact of nephrolithiasis on renal function is poorly understood, primarily due to reasonable limitations placed on performing invasive medical procedures in marine mammals. The purpose of this study was to evaluate ^{99m}TC-MAG3 as an agent to measure renal function in dolphins.

Methods: Renal scintigraphy utilizing ^{99m}TC-MAG3 was performed in nine dolphins in a case-controlled study. Three control dolphins had no historical evidence of renal disease on blood or urine. Six case dolphins had clinical histories of episodic azotemia, hematuria, and ultrasound evidence of nephrolithiasis. Animals were transported to the University of California San Diego Medical Center, sedated with an intramuscular injection of midazolam (0.07 – 0.09 mg/kg), and injected with 1110-1370 MBq (30-37 mCi) of ^{99m}TC-MAG3 in the caudal peduncle periarterial venous rete. Dynamic acquisition studies consisted of two seconds per frame for the first 58-60 seconds after injection, followed by one minute per frame for the next 25-30 minutes.

Results: Two control animals had renograms and associated time activity curves (TAC) similar to normal renograms seen in humans and companion animals. There was symmetrical distribution of radiopharmaceutical uptake with a well-defined vascular phase followed by a nephrographic phase, and clear visualization of the kidneys from the background tissues. One control animal had delayed peak uptake in the abdominal aorta when compared to the other dolphins, likely due to an inadequate bolus of the radiopharmaceutical. All cases had abnormal renograms and TACs when compared to controls. Abnormalities included asymmetric radiopharmaceutical uptake, where cases were more likely than controls to have asymmetric uptake ($P=0.03$). Additional abnormalities included delayed radiopharmaceutical uptake in both the vascular and nephrographic phases and photopenic defects on the perfusion and nephrographic images. No behavioral or physiologic adverse effects were seen post-procedure.

Discussion/Conclusion: A technique was developed to perform ^{99m}TC-MAG3 renal scintigraphy in bottlenose dolphins. The radiopharmaceutical was considered to be safe in all animals. Renograms in control dolphins were similar to normal renograms in humans and companion animals. Abnormal renograms were seen in animals with histories of hematuria, episodic azotemia, and ultrasound evidence of nephrolithiasis.

TECHNETIUM 99m THYROID TO BACKGROUND (T:B) RATIOS FOR FELINE ^{131}I TREATMENT SUCCESSES AND FAILURES USING 4 mCi I-131.

S.T. Wallack[1], M. Metcalf[1], A. Skidmore[1], C. Lamb[2]. Veterinary Imaging Center of San Diego, CA, 92111[1]. The Royal Veterinary College, UK, AL9 7TA[2].

Introduction/Purpose: Standard dosing of 4 mCi for the treatment of feline hyperthyroidism is common. A 4 mCi dose has been documented to have a 94-98% cure rate. In people, treatment failures for therapy have been associated with inadequate ^{131}I dosage, large goiter volume and a higher T_3 or T_4. Similar associations have been seen in cats. The objective of this study was to evaluate the thyroid to a standardized background ROI on the pre-treatment thyroid scan to obtain a thyroid to background (T:B) ratio.

Method: This is a retrospective study in which six (6) ^{131}I treatment failures and one hundred seven (107) ^{131}I treatment successes were compared. All cats underwent a pre-treatment pertechnetate thyroid scan using 3.0 mCi the day of ^{131}I treatment. Within 4 hours of the thyroid scan, these patients received a subcutaneous injection of 4 mCi of ^{131}I. T_4 and renal values were measured at 1, 3, 6 and 12 months following ^{131}I therapy. A treatment failure was defined by a continued elevation in T4 and residual overactive thyroid tissue, in the same location as pre-treatment, on a follow-up pertechnetate thyroid scan. The thyroid to background ratio (T:B) was performed on the initial pre-treatment thyroid scan using Mirage software and the A/B ratio. All thyroid scans were measured with the color palette set to aqua marine which resulted in a distinct aqua border around the overactive thyroid tissue. The background ratio was the default circle placed over the left or right axillary region. The thyroid tissue was manually traced along the outer margin of the aqua marine colored thyroid activity. All thyroid scans in this study demonstrated round, smoothly marginated lesions in the region of the thyroid gland with no evidence of ectopic thyroid tissue. Biopsy confirmation was not performed.

Results: Results in 107 (95%) cats treated successfully were compared with results in 6 (5%) cats that remained hyperthyroid after treatment. T:B ratio was significantly higher for cats that had treatment failure (median 13.0, range 3.6-73.0) than for cats treated successfully (median 4.4, range 1.2-69.0) ($p=0.02$), whereas there was no significant difference in their T:S ratios ($p=0.2$) or pre-treatment serum T4 concentration ($p=0.47$). Odds ratio of treatment failure using fixed dose ^{131}I treatment rose as the T:B ratio became higher.

Discussion/Conclusion: The findings suggest a trend towards a higher T:B ratio in ^{131}I treatment failures using a 4 mCi dose with a suspected adenoma. Other factors could be thyroid size, patient weight, sex, age, methimazole dosage, methimazole withdrawal time prior to therapy, length of methimazole treatment, time from diagnosis to radioiodine treatment, and T_4. The thyroid scan may be useful as a pretreatment test to identify cats that may require more than 4 mCi of ^{131}I to successfully treat feline hyperthyroidism.

FELINE ^{131}I TREATMENT SUCCESSES AND FAILURES USING A DUAL DOSING PROTOCOL OF 4 mCi OR 7 mCi I-131 BASED ON THE T:B RATIO.

S.T. Wallack[1], A. Bettencourt[1], J. Balairon[1], C. Lamb[2]. Veterinary Imaging Center of San Diego, CA, 92111[1]. The Royal Veterinary College, UK, AL9 7TA[2].

Introduction/Purpose: Standard dosing of 4 mCi for treatment of feline hyperthyroidism is standard practice. A 4 mCi dose has been documented to have a 94-98% cure rate with a more typical first time treatment failure rate of 5%. In people, treatment failures for therapy have been associated with inadequate ^{131}I dosage, large goiter volume and a higher T_3 or T_4. Similar associations have been seen in cats. Recent research has indicated that the odds ratio of treatment failure using fixed dose ^{131}I treatment rose as the thyroid to background (T:B) ratio became higher. Treatment success rate was evaluated when treatment dosage was increased to 7mCi when the T:B ratio was 11 or greater.

Methods: This was a prospective study in which two hundred twelve (212) confirmed hyperthyroid cats were treated with either 4mCi or 7 mCi ^{131}I. All cats underwent a pre-treatment pertechnetate thyroid scan using 3.0 mCi the day of ^{131}I treatment. All cats had both a thyroid to salivary (T:S) ratio and a thyroid to background (T:B) ratio calculated. ^{131}I dosing was determined from the T:B ratio. Cats with a T:B ratio <11 were administered 4 mCi subcutaneously and cats with a T:B ratio equal to or > 11 were administered 7 mCi. Actual dose was within 10% of supplied dose by ^{131}I supplier. In equivocal cases where the T:B ratio was measured several times the highest T:B ratio was used to guide treatment. Within 4 hours of the thyroid scan, these patients received ^{131}I treatment. T_4 and renal values were measured at 1, 3, 6 and 12 months following ^{131}I therapy. A treatment failure was defined by continued elevation in T4 over the following 12 months. The thyroid to background ratio (T:B) was performed according to the previously described protocol for T:B ratio calculation. All thyroid scans in this study demonstrated round, smoothly marginated lesions in the area of the thyroid gland with no evidence of ectopic thyroid tissue. Biopsy confirmation was not performed.

Results: Two hundred seven (97.64%) cats were treated successfully and 5 (2.63%) cats remained hyperthyroid after treatment. Thirty eight cats (17.93%) were hypothyroid at 12 months following treatment. Of the hypothyroid cats, seven of the 37 (18.9%) hypothyroid cats were on thyroid hormone supplementation and 1 of 37 (2.70%) was likely on hormone supplemental therapy but this could not be confirmed. Of all cats treated, 3.77% were on thyroid supplementation for permanent hypothyroidism.

Discussion/Conclusion: The findings suggest a high success rate for first time ^{131}I treatment when using a 4 mCi or 7 mCi ^{131}I treatment protocol that is based upon the pre-treatment T:B ratio cut-off of 11. Reasons for the non-responders is unknown at this time and could be due to thyroid size, patient weight, sex, age, methimazole dosage, methimazole withdrawal time prior to therapy, length of methimazole treatment, time from diagnosis to radioiodine treatment, and pre-treatment T_4. The thyroid scan may be useful not only as a pre-treatment test to confirm hyperthyroidism but also to determine which cats may require more than 4 mCi ^{131}I to successfully treat feline hyperthyroidism.

OPTIMIZATION OF SMALL ANIMAL DIGITAL RADIOGRAPHIC TECHNIQUE TO MAXIMIZE SIGNAL TO NOISE AND EVALUATE THE EFFECTS ON PERSONNEL EXPOSURE.

C.N. Copple, I. D. Robertson, and D. E. Thrall. North Carolina State University, North Carolina, 27606

Introduction/Purpose: With digital radiography systems, a wide range of kVp and mAs combinations can be used to produce interpretable images. However, this wide range can lead to unnecessary patient and personnel exposure or noisy images. Most vendors provide technique chart for their digital imaging plates but veterinarians may still not know the optimal exposure factors to use for a specific imaging study. Defining optimal kVp and mAs values for a digital imaging plate has been evaluated in human radiography but there is a need to optimize exposure factors for veterinary radiography using a digital plate. This is the first study in veterinary medicine thus far to address optimization of exposure factors of a digital imaging system.

Methods: A single exposure technique was used to calculate the optimal radiographic exposure factors for a test range of kVp values, using a range of phantom thicknesses. Optimization was based on a published benchmark [(signal difference to noise ratio)^2/exposure]. Personnel exposure was used as the denominator. The kVp values assessed were 60, 81, 100, and 121. Phantom thicknesses were 2cm, 5cm, 10cm, 15cm, 20cm, 25cm, and 30cm. The mAs range for each kVp and phantom thickness also varied, but was clinically relevant. Acrylic blocks and plexiglass waterbaths were used as tissue-equivalent phantoms. Simulated lesions of soft tissue and bone equivalent material were placed on the phantoms, providing regions of interest in which to measure the pixel intensity of the detector signal. Personnel radiation at a specified distance of ~40cm was measured with an ion chamber to provide unit exposure data in mR. Using this method, the optimal technique is the one that produced the highest resulting figure of merit.

Results: For all 7 patient thicknesses tested, the figure of merit was different for each thickness. This indicates that it is not appropriate to use a single standard radiographic technique for all patients using a digital plate and that a technique chart based on patient thickness ranges needs to be established. Our data are useful for establishment of this technique chart.

Discussion/Conclusion: The objective method of determining figure of merit shows that a single standard technique is not optimal for the various patient thicknesses imaged in veterinary medicine, especially when accounting for the lowest personnel exposure. Given that the figure of merit is dependent on technique, technique should be optimized for defined ranges of patient thickness.

TRAINING RESIDENTS TO WRITE MEANINGFUL REPORTS.

P.V. Scrivani, N.L. Dykes, M.S. Thompson, A.E. Yeager. Cornell University, NY 18453

Introduction/Purpose: A critical task of radiologists is writing accurate, concise, and easily understood reports. Effective reporting is becoming even more important as the increased use of teleradiology and remote interpretation become more prevalent. Meaningful reports do not only list abnormalities and differential diagnosis but also prevent errors by improving understanding of findings relative to the particular patient and influencing care givers to perform the appropriate next steps. Thus, helpful report writing is a core skill to emphasize during training and may be improved if consistent feedback from experienced mentors is readily available. To accomplish this task, we developed web-based software that augments the existing RIS functionality of our hospital management software (UVIS) in two key areas. The primary purpose was to provide our residents with side-by-side review of draft and final reports. This comparison between resident and faculty versions of the report allows identification of omitted or excessive information and style changes to be incorporated into future reports. Second, this program stores the draft reports, which are not retained in the UVIS database after faculty edits are applied, since actions may have been taken based on the draft interpretation. The purpose of this abstract is to demonstrate the software and report the statistics automatically gathered during the first year of use.

Methods: Data were extracted via the "Dashboard" function of the program. Percentages of cases reviewed by modality, species, time-to-report, and time-to-acknowledge per resident were gathered.

Results:

From July 2009 to March 2010, the total number of final reports was 5685. The average time to create preliminary reports was 1.75 (SD, 5.9) days with an average time to finalization of 3.8 (SD, 9.7) days. The total average time to produce final reports for all users (residents and radiologists) was 6.3 (SD, 14.9) days. At the time of abstract submission, 61% of reports have been acknowledged by the resident.

RESIDENT	CR SA	CR LA	CT	MR	NM	RF	US	TOTAL
First-year (A)	683	192	85	28	24	18	0	1030
First-year (B)	763	225	121	24	27	23	0	1183
Second-year	735	150	56	26	21	15	350	1353
Third-year	397	80	53	17	12	8	545	1112
TOTAL	**2578**	**647**	**315**	**95**	**84**	**64**	**895**	**4678**

Discussion/Conclusion: We now have a mechanism for providing consistent automated feedback on every case written by residents and reviewed by faculty. Future work will include tracking residents' reports for content and style progress. Data also provide benchmark values for quality control regarding workload and report generation by the Section.

Wednesday, August 18, 2010 ***(ACVR and RO simultaneous sessions)***

RO

9:00 am	**Radiation Oncology Scientific Session 3: Round Table Discussion**	Roosevelt KL
10:00 am	*Break with Exhibitors*	Grand Ballroom B
10:30 am	RO Business Meeting	
12:00 pm	*Buffet Lunch*	Grand Ballroom C
1:00 pm	Resident Authored Paper and Grant Awards	
1:10 pm	ACVR Image Interpretation Session	

Thursday, August 19, 2010

7:00 am **Large Animal Diagnostic Imaging Society Meeting** — Grand Ballroom A

7:30 am *Registration opens* — Vanderbilt Registration

8:00 am CT/MRI Society Keynote Address
Advances in MRI for Microimaging and Cell Tracking
Dr. Paula Foster

9:00 am **ACVR Scientific Session 6: CT/MRI**
Moderator: Dr. Shannon Holmes

9:00 am **Measurement of Normal Canine Adrenal Gland Size on Transverse Plane in CT.**
K.S. Clapp, R. Drees. University of Wisconsin-Madison School of Veterinary Medicine, Department of Surgical Sciences, Wisconsin, 53706.

9:15 am **Comparison of Adrenal Gland Dimensions and Volume with MRI and Ultrasound in 7 Cadaver Dogs.**
J.L.F. Hayles, R.L. Tucker, J.M. Gay. Washington State University, WA 99164

9:30 am **Accuracy of Computed Tomography in Determining Lesion Size in Canine Osteosarcoma of the Appendicular Skeleton.**
K. S. Karnik, E. M. Green, V. F. Samii, S. E. Weisbrode, C. A. London. The Ohio State University, OH 43210

9:45 am **Low-field MR imaging of meniscal tears in dogs: Variations in diagnostic performance of observers.**
P. Böttcher[1], L. Armbrust[2], L. Blond[3], A. Brühschwein[4], P.R. Gavin[5], I. Gielen[6], S. Hecht[7], K. Jurina[8], S. Kneissl[9], M. Konar[10], E. Pujol[11], A. Robinson[12], S.L. Schaefer[13], L.F.H. Theyse[14], A. Wigger[15], E. Ludewig[1]. [1]University of Leipzig, Leipzig 04103 Germany, [2]Kansas State University, KS 66506, [3]Université de Montréal, J2S 7C6 Canada, [4]Ludwig-Maximilians-University, Munich 80539, Germany, [5]Washington State University, WA 99164, [6]Ghent University, Ghent 9000, Belgium, [7]University of Tennessee, TN 37996, [8]Tierklinik Haar, Haar 85540, Germany, [9]University of Veterinary Medicine, Vienna 1210, Austria, [10]MRI support service, Ripa di Seravezza, 55047, Italy, [11]CHV Fregis, Arcueil 94110, France, [12]Dovecote Veterinary Hospital, Castle Donington DE74 2LJ, UK, [13]University of Wisconsin-Madison, WI 53706, [14]University Utrecht, Utrecht 3508TC, Netherlands, [15]Justus-Liebig-University, Giessen 35390, Germany.

10:00 am *Break with Exhibitors* — Grand Ballroom B

Thursday, August 19, 2010

10:30 am **ACVR Scientific Session 7: CT/MRI**
Moderator: Dr. John Hathcock

10:30 am **Diffusion Tensor Imaging in the Canine Spinal Cord.**
A.P. Pease, R. Miller. College of Veterinary Medicine, Michigan State University, East Lansing, MI. 48824.

10:45 am **Magnetic Resonance Imaging Features of Astrocytic and Oligodendroglial Tumors in Dogs.**
B.D. Young[1], J.M. Levine[1], B.F. Porter[1], A.V. Chen-Allen[2], J.H. Rossmeisl[3], S.R. Platt[4], M. Kent[4], G.T. Fosgate[5], S.J. Schatzberg[4].
[1]Texas A&M University, College Station, TX, [2]Washington State University, Pullman, WA, [3]Virginia Tech, Blacksburg, VA, [4]University of Georgia, Athens, GA, and [5]University of Pretoria, Onderstepoort, South Africa

11:00 am **Magnetic Resonance Lymphography (MR-LG) Techniques in Canine Patients with Cases Examples.**
S.P. Holmes,[1] C.W. Schmeidt,[1] E.B. Cohen[1] & N.J. Bacon[2] University of Georgia College of Veterinary Medicine, Georgia, 30602 & University of Florida, Gainesville, 32610.

11:15 am **Reliability of Sagittal T2-Weighted Alone or Combined with Single-Shot Fast Spin Echo Sequences for Detecting Sites of Disc Herniation in 120 Dogs.**
R. Guillem, J. Suran, A.V. Caceres, J.A. Reetz, W. Mai. From the University of Pennsylvania, Philadelphia, PA 19104.

11:30 am **A Protocol and Early Experience with Magnetic Resonance Imaging for Pericardial Disease and Cardiac Masses in Dogs.**
Fischetti AJ, Trafny D, Fox PR. Animal Medical Center, New York, NY 10065.

11:45 am **Imaging of Coronary Arteries Using 64-Slice MDCT Angiography in the Dog.**
R. Drees[1], A.P. Frydrychowicz[2], S.B.Reeder[2-5], M.E. Pinkerton[6], R. Johnson[1]

12:00 pm *Buffet Lunch* Grand Ballroom C

1:00 pm **ACVR Scientific Session 8: CT/MRI**
Moderator: Dr. Shannon Holmes

Thursday, August 19, 2010

1:00 pm **Labeling of Equine Umbilical Cord Blood-derived MSCs with SPIO Contrast Medium and in Vivo Detection with MRI.**
R Cruz – Arámbulo,[1] P Foster[2], DH Betts[1,3], TG. Koch, [1,4]
(1) University of Guelph, Ontario, Canada N1G2W1 (2) Imaging Research Laboratories, Robarts Research Institute, London, Ontario, Canada N5X4K8 (4) University of Western Ontario, London, Ontario, Canada N6G 1G9 (3) Orthopaedic Research Lab. Aarhus University, Denmark

1:15 pm **MRI Findings in the Equine Stifle of the Performance horse and Correlation with the Human Knee.**
A.L. McKnight[1], K.E. Kreider[2], C.A. Dolinskas[3], J.C. Posh[4], H.T. Stevens[2], S.D. Bennett[5] McKnight Insight, PA 19317[1]; Equine Services, FL 33414[2]; Pennsylvania Hospital, PA 19107[3]; Univ. of Pennsylvania, PA 19104[4] Equine Services, KY 40067[5]

1:30 pm **ACVR Scientific Session 9:**
Poster Session with Authors Grand Ballroom B

Cross-Sectional Pathology Amends Cross-Sectional Imaging.
S. Kneissl, A. Fuchs-Baumgartinger, A. Probst. University of Veterinary Medicine, Vienna, Austria, A 1210.

CT Evaluation of Oblique Spinous Processes in Dogs and Cats.
S. Kuzmits, C. Semeliker, A. Probst, A. Tichy, S. Kneissl. University of Veterinary Medicine, Vienna, Austria, A 1210.

Susceptibility Artifacts Due to Metallic Foreign Bodies in Small Animal MRI.
S.Hecht, W.H.Adams, J.Narak, W.B.Thomas
Department of Small Animal Clinical Sciences, University of Tennessee College of Veterinary Medicine, Knoxville, TN, USA

Magnetic Resonance Imaging of the Feline Hippocampus.
Francis KA, Drost WT, Schmalbrock P, Burns P, Buffington CAT. The Ohio State University, Veterinary Medical Center and Wright Center of Biomedical Innovation, Columbus, OH 43210.

Evaluation of Ergonomic Risk Factors Among Veterinary Sonographers.
E.K. Randall, D.P. Gilkey, A.A. Patil, J.C. Rosecrance, D.I. Douphrate.
Colorado State University, Fort Collins, CO, 80526.

Thursday, August 19, 2010

1:30 pm **ACVR Scientific Session 9:**
Poster session with Authors Grand Ballroom B

Lack of Associations Between Ultrasonographic Appearance of the Canine Liver and Histologic Diagnosis.
C.M.R. Warren-Smith, S. Andrew S, C.R. Lamb. The Royal Veterinary College, University of London, Hertfordshire AL9 7TA, U.K.

Diagnostic Veterinary Imaging Using Micro-Imaging Platforms.
J. S. Wall, A. Stuckey, S. J. Kennel, T. Richey, [1]F. Morandi, [1]M. Jones, [1]C Greenacre, [2]M. Souza, and [1]A. LeBlanc. University of Tennessee Graduate School of Medicine, Knoxville, TN; [1]Departments of Small Animal Clinical Sciences and [2]Comparative Medicine, University of Tennessee College of Veterinary Medicine, Knoxville, TN, 37922.

Initial Experience with the Classroom Performance System™ (CPS™) in Radiology Education.
S.Hecht[1], W.H.Adams[1], M.A.Cunningham[2], I.F.Lane[1]
[1]Department of Small Animal Clinical Sciences and [2]Instructional Resources, University of Tennessee College of Veterinary Medicine, Knoxville, TN, USA

2:30 pm *Break with Exhibitors* Grand Ballroom B

2:45 pm Large Animal Diagnostic Imaging Society Keynote Address
Equine Tendon and Ligament Injuries
Dr. Norm Rantanen

4:45 pm *Adjourn and Exhibitors close*

MEASUREMENT OF NORMAL CANINE ADRENAL GLAND SIZE ON TRANVERSE PLANE IN CT.

K.S. Clapp, R. Drees. University of Wisconsin-Madison School of Veterinary Medicine, Department of Surgical Sciences, Wisconsin, 53706.

Introduction/Purpose: Normal limits for canine adrenal gland size have been established anatomically and ultrasonographically. Estimation of adrenal gland size with CT has recently been proposed using the volumetric measurements of 0.60cm^3 for the left and 0.55 cm^3 for the right adrenal. However, performing this measurement may be limited in practice on a daily basis due to time and software constraints. Because the canine adrenal glands are usually not parallel to the long axis of the dog, it is probable that a measurement of width or height performed on transverse plane CT images would be inadequate due to orientation of the adrenal gland to the transverse scan plane or effects of partial volume artifact. The purpose of this study was to test if width or height measurements of the cranial and caudal poles of the normal canine adrenal glands would result in values within the reported normal range or produce falsely enlarged measurements.

Methods: In this retrospective study, CT scans of 51 dogs with no signs of adrenal disease were used. Imaging studies were performed with the patients in dorsal or ventral recumbency on a single detector row computed tomography unit using helical acquisition mode, medium frequency reconstruction algorithm, 2-5mm slice thickness and helical reconstruction interval. Using electronic calipers a measurement was obtained in the orientation most closely resembling the widest dorsal (width) and sagittal (height) plane of the cranial and caudal poles of the left and right adrenal each.

Results: Measurement of the width of the cranial and caudal pole of the left and right adrenal gland resulted in values compatible with and commonly smaller than reported normal values. Only a few height measurements of the caudal pole of the left and right adrenal gland were above the reported normal range. Measurement of the height of the cranial pole of the left and right adrenal gland almost always resulted in values above the reported normal values.

Discussion/Conclusion: Measuring adrenal gland size on transverse CT images using an orientation most closely resembling the dorsal plane (width) of the cranial and caudal pole of the right and left adrenal will result in values in the reported reference ranges where as measurements in an orientation most closely resembling the sagittal plane (height) can result in values above the reference range for the cranial and caudal pole of the left and right adrenal gland.

COMPARISON OF ADRENAL GLAND DIMENSIONS AND VOLUME WITH MRI AND ULTRASOUND IN 7 CADAVER DOGS.

J.L.F. Hayles, R.L. Tucker, J.M. Gay. Washington State University, WA 99164

Introduction/Purpose: Ultrasound evaluation of canine adrenal glands is routine in canine abdominal ultrasonography. Despite numerous publications attempting to quantify and standardize adrenal gland size in dogs, ultrasonic evaluation of adrenal glands remains subjective. Attempts to objectively evaluate adrenal gland size in comparison to surrounding internal markers have shown moderate correlation. MR imaging of normal canine adrenal glands has been described. The purpose of this study was to compare the dimensions and volume of adrenal glands between ultrasound and MRI, relative to actual adrenal gland size and volume.

Methods: Seven healthy mixed breed dogs were euthanized and all imaging and gross adrenal gland measurements were performed within 24 hours. Ultrasonography was performed with a 4-13 MHz linear transducer (Biosound Esaote MyLab 70). MRI was performed with a 1T Philips Gyroscan and transverse, dorsal and sagittal imaging planes were acquired. T2-Wt images provided maximum adrenal gland contrast with the surrounding retroperitoneal fat. All glands were clearly identified with both imaging modalities. Linear measurements with both ultrasound and MRI included: maximum cranial and caudal pole diameter and maximum length. Following imaging, the adrenal glands were harvested and gross linear measurements were recorded. Two sonographic techniques were used to estimate adrenal volume: elliptical and trace volume estimation. MRI volume estimation was acquired with 3D imaging software (3D-DOCTOR, Able Software Corp.). MRI adrenal gland volume was estimated with transverse, dorsal and sagittal images. Volume measurement of the actual adrenal glands was based on volume displacement.

Results: Using linear regression, moderate to good correlation was found between both linear and volume estimation with MRI in comparison to the actual adrenal gland measurements (cranial pole: adj.r^2=0.578, p=0.001, caudal pole: adj.r^2=0.380, p=0.011, length: adj.r^2=0.738, p=<0.001, volume: adj.r^2=0.872, p=<0.001). Poor correlation was found with ultrasound adrenal pole measurements and volume estimates. Maximum adrenal gland length measured with ultrasound had moderate correlation with the actual glands. Adrenal glands were judged to be normal on histologic examination.

Discussion/Conclusion: In a small number of cadaver dogs, this study demonstrated MRI is useful in objectively determining adrenal gland dimensions and volume. Ultrasound underestimated maximum cranial and caudal adrenal gland diameters and proved inaccurate for determining adrenal gland volume. Further MRI evaluation of canine adrenal glands is needed to establish normal and abnormal linear and volumetric values and their relationship to body size and clinical significance.

ACCURACY OF COMPUTED TOMOGRAPHY IN DETERMINING LESION SIZE IN CANINE OSTEOSARCOMA OF THE APPENDICULAR SKELETON.

K. S. Karnik, E. M. Green, V. F. Samii, S. E. Weisbrode, C. A. London. The Ohio State University, OH 43210

Introduction/Purpose: Osteosarcoma (OSA) is the most common bone neoplasm in dogs and is associated with rapid progression of metastasis and high rate of mortality. Recent studies have investigated the accuracy of measuring the extent of appendicular OSA lesions using computed tomography (CT), nuclear scintigraphy, radiography, and magnetic resonance imaging. All of these modalities overestimated the extent of disease.

To our knowledge, use of multi-detector CT technology performed before and after intravenous contrast medium administration to identify the extent of appendicular OSA has not been performed in the dog. Multi-detector technology with sub-millimeter acquired images allows for more precise measurements to be made compared to previous studies. The goal of this study is to assess the extent of appendicular OSA with multi-detector contrast enhanced CT and compare that with the gold standard of histopathology. Accurately determining the extent of diseased bone is of importance for surgical margins in limb-spare procedures and also in serial monitoring of response of diseased bone to chemotherapy or radiation therapy when amputation is not performed.

Methods: Osteosarcoma was confirmed following biopsy post amputation of all limbs. Dogs with a pathological fracture or prior chemotherapy/radiotherapy were excluded. A series of 0.625 mm transverse contiguous images of the affected and contralateral limb were acquired before and after intravenous contrast medium administration prior to surgical amputation. Linear and volume measurements were made from acquired and reformatted CT images. The extent of disease was confirmed with histopathologic evaluation of the limb following amputation.

Results: Compared to histopathology, CT underestimated the extent of disease by 7.23 mm (10.27%) in one patient and by 15.60 mm (17.83%) in another.

Discussion/Conclusion: Multi-detector contrast enhanced CT may underestimate the extent of OSA of the appendicular skeleton. It may still be valuable in assessing progression/regression of response to chemotherapy or radiotherapy, however additional studies should be performed for further evaluation. With a limb spare procedure, multi-detector CT may be valuable in recognizing the minimum extent of disease and ensuring the surgeon obtains larger margins.

LOW-FIELD MR IMAGING OF MENISCAL TEARS IN DOGS: VARIATIONS IN DIAGNOSTIC PERFORMANCE OF OBSERVERS.

P. Böttcher[1], L. Armbrust[2], L. Blond[3], A. Brühschwein[4], P.R. Gavin[5], I. Gielen[6], S. Hecht[7], K. Jurina[8], S. Kneissl[9], M. Konar[10], E. Pujol[11], A. Robinson[12], S.L. Schaefer[13], L.F.H. Theyse[14], A. Wigger[15], E. Ludewig[1]. [1]University of Leipzig, Leipzig 04103 Germany, [2]Kansas State University, KS 66506, [3]Université de Montréal, J2S 7C6 Canada, [4]Ludwig-Maximilians-University, Munich 80539, Germany, [5]Washington State University, WA 99164, [6]Ghent University, Ghent 9000, Belgium, [7]University of Tennessee, TN 37996, [8]Tierklinik Haar, Haar 85540, Germany, [9]University of Veterinary Medicine, Vienna 1210, Austria, [10]MRI support service, Ripa di Seravezza, 55047, Italy, [11]CHV Fregis, Arcueil 94110, France, [12]Dovecote Veterinary Hospital, Castle Donington DE74 2LJ, UK, [13]University of Wisconsin-Madison, WI 53706, [14]University Utrecht, Utrecht 3508TC, Netherlands, [15]Justus-Liebig-University, Giessen 35390, Germany.

Introduction/Purpose: To evaluate multiobserver diagnostic performance and reader agreement for meniscal tear detection using low-field MRI (lfMRI) in dogs with suspected cranial cruciate ligament disease, with arthroscopy as the reference standard.

Methods: 50 lfMR studies were reviewed independently for presence or absence of meniscal tear lesion by 15 observers representing 5 levels of experience. Each stifle had 7 predefined lfMRI sequences using a 0.5 Tesla magnet and human knee coil. Sensitivity, specificity, positive predictive value (PPV), negative predictive value (NPV), and accuracy were calculated for each observer for each stifle and for medial menisci (MM) and lateral (LM). Level of observer experience was rated according to number of stifles evaluated before. Differences in diagnostic performance of the individual observer and level of experience were statistically analysed. Inter-rater agreement was based on intra-class correlation coefficient (ICC) analysis.

Results: Overall accuracy was 80% for MM tears and 92% for LM tears. Median sensitivity for MM tears was 74% and specificity 89%. For LM tears, median sensitivity was 33% and specificity 94%. PPV and NPV were 83% and 79%, respectively, for MM tears, and 94% and 92% for LM tears. No association was found between level of experience and diagnostic performance of individual observers ($p > 0.05$). Inter-rater agreement was low for normal menisci (ICC 0.13, 95% CI 0.08, 0.20) and moderate for injured menisci (ICC 0.50, 95% IC: 0.36, 0.67).

Discussion/Conclusion: Depending on the observer, lfMRI is insufficiently accurate meniscal tears in dogs to be considered a useful method of assessment. Moderate accuracy and low to moderate inter-rater agreement suggest that a consensus based on dual-reading of images should be considered for clinical lfMRI studies of the canine stifle.

DIFFUSION TENSOR IMAGING IN THE CANINE SPINAL CORD.

A.P. Pease, R. Miller. College of Veterinary Medicine, Michigan State University, East Lansing, MI. 48824

Introduction/Purpose: Diffusion tensor imaging (DTI) is a magnetic resonance imaging sequence performed to evaluate the random motion of water molecules. Based on water motion, the data can be analyzed to determine if the water is freely moving or if axons are present causing restriction of the random water motion. In humans, this technique is used as an anatomic guide to determine the orientation of axons in the spinal cord as well as evaluating displacement or destruction of axons for the purpose of prognosis. To date, this method for spinal cord evaluation has not been performed in veterinary patients. Our hypothesis is that DTI can be used as method to evaluate the spinal cord in dogs and determine if axon degeneration is present.

Methods: Eleven clinically normal Beagle dogs and 6 dogs with clinical lesions localized to the spinal cord were enrolled in this study. Dogs were considered normal based on physical examination and normal T1 and T2 weighted MR images of the spinal cord. The 6 abnormal dogs presented to MRI for lesions localized to the spinal cord and DTI images were obtained as part of the MR imaging exam. All scans were performed with a 1.5T Siemens Espree magnetom using a spinal coil and 20 image planes. After the scan was complete, DTI images were processed using specialized imaging software (Siemens Neuro3D) to evaluate the axons using fiber tracking.

Results: The 11 normal Beagle dogs were approximately 2 years of age and had uniform linear axons seen within the spinal cord. The fibers were all traveling in a craniocaudal direction and nerve roots could be seen exiting the intervertebral foramen. The 6 abnormal dogs were between 2 and 10 years of age. Three dogs were diagnosed with intervertebral disc disease, one with intradural-extramedullary spindle cell tumor, one was presumed to have a fibrocartilageneous emboli, and one dog had Clostridial osteomyelitis and myelomalacia. (Figure 1) Nerve fiber tracking allowed for the observation of deviation of the spinal cord axons on all of the extradural and intradural-extramedullary lesions and showed a decreased number of nerve fibers in the dog with Clostridial myelomalacia.

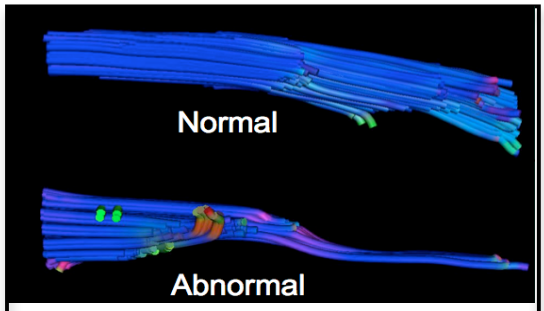

Figure 1: DTI images showing a normal spinal cord (above) and a spinal cord with myelomalacia (below)

Discussion/Conclusion:
Diffusion tensor imaging can be performed in the spinal cord of dogs and provides information on axonal degeneration and axonal loss as seen with myelomalacia. Further studies are needed to determine if information on prognosis can be obtained similar to recent studies in humans with chronic disc herniations.

MAGNETIC RESONANCE IMAGING FEATURES OF ASTROCYTIC AND OLIGODENDROGLIAL TUMORS IN DOGS.

B.D. Young[1], J.M. Levine[1], B.F. Porter[1], A.V. Chen-Allen[2], J.H. Rossmeisl[3], S.R. Platt[4], M. Kent[4], G.T. Fosgate[5], S.J. Schatzberg[4]. [1]Texas A&M University, College Station, TX, [2]Washington State University, Pullman, WA, [3]Virginia Tech, Blacksburg, VA, [4]University of Georgia, Athens, GA, and [5]University of Pretoria, Onderstepoort, South Africa.

Introduction/Purpose: Magnetic resonance (MR) imaging is the modality of choice for evaluating central nervous system structures. Although glial (astrocytic and oligodendroglial) neoplasias represent 40-70% of histologically confirmed canine brain tumors, their MR appearance has been characterized in case reports or small case series. The purpose of this study was to describe the antemortem MR imaging features of histologically confirmed, intracranial astrocytic and oligodendroglial tumors in a multi-center population of dogs.

Methods: The medical records of 37 dogs from four institutions that had an intra-axial brain mass identified on antemortem MR imaging and had a histologic diagnosis of glioma were reviewed. Original brain tissue samples obtained either from necropsy or biopsy from each case was re-examined by a single pathologist to confirm tumor type. Special stains were applied to determine tumor grade, according to the World Health Organization (WHO) classification system. Thirty animals were re-confirmed to have astrocytomas (14) or oligodendrogliomas (16). The MR images from these dogs were evaluated independently for predetermined MR characteristics by two authors, blinded as to tumor type. Consensus agreement was reached for all data points. Imaging characteristics were compared between tumor type and grades using chi-square or Fisher exact tests.

Results: All of the oligodendrogliomas and 12 astrocytomas were located in the cerebrum or thalamus, with the remainder of astrocytomas in the cerebellum or caudal brainstem. Most (27/30) tumors were associated with both grey and white matter. The signal characteristics of both tumor types were hypointense on T1W (12 each) and hyperintense on T2W (11/14 astrocytomas, 12/16 oligodendrogliomas) images. The remaining cases were of mixed intensity. For astrocytomas and oligodendrogliomas, respectively, common findings were contrast enhancement (10/14, 11/16), peripheral rim contrast enhancement (6/14, 9/16), hemorrhage (4/14, 6/16), and cystic regions within the mass (7/14, 10/16). Caudal transtentorial herniation (7/14, 10/16) and foramen magnum herniation (5/14, 3/16) also were commonly associated with astrocytomas and oligodendrogliomas, respectively. Interestingly, contact with some margin of the lateral ventricle was the most common finding, occurring in 13/14 astrocytomas and 14/16 oligodendrogliomas.

Discussion/Conclusion: Magnetic resonance imaging signal and enhancement characteristics of astrocytomas and oligodendrogliomas were similar. Both tumor types contacted the lateral ventricles and were associated with a high rate of brain herniation. Further studies are needed to differentiate between these glial neoplasms on MR.

MAGNETIC RESONANCE LYMPHOGRAPHY (MR-LG) TECHNIQUES IN CANINE PATIENTS WITH CASE EXAMPLES.

S.P. Holmes,[1] C.W. Schmeidt,[1] E.B. Cohen[1] & N.J. Bacon[2] University of Georgia College of Veterinary Medicine, Georgia, 30602 & University of Florida, Gainesville, 32610

Introduction/Purpose: Current diagnostic imaging of the lymphatic system includes iodinated contrast radiography, computed tomography, and radiolabelled colloid scintigraphy. Magnetic resonance lymphography (MR-LG) avoids many shortcomings of these modalities via multiplanar imaging and superior contrast resolution, and allowing visualization of pathology in surrounding soft tissues. It is currently employed in human medicine as a primary imaging modality. This report is the first to describe the veterinary application of two MR-LG techniques, heavily T2-weighted imaging and contrast-enhanced interstitial MR-LG, as well as examples of lymphatic pathology on MR-LG.

***Methods*:** MR-LG was performed on the thoracic limbs of three normal control dogs (patients 1-3), one dog with lymphatic obstruction secondary to previous axillary surgical cicatrix (patient 4), and one dog with congenital lymphangiomatosis (patient 5). Patients 1-4 were imaged with a GE HDX 3.0T Sigma twin gradient MRI; the 5th patient was imaged with a Toshiba Vantage 1.5T MRI. Body matrix or phased array spine coils were used to accommodate different patient sizes. Patients 1, 2, 3 and 5 were positioned in sternal recumbency with thoracic limbs extended. Patient 4 was positioned in lateral recumbency, as the affected limb would not extend further than perpendicular to the thorax. Routine MR sequences to evaluate thoracic limb pathology were performed prior to MR-LG. Both MR-LG techniques, heavily T2-weighted images and contrast-enhanced interstitial MR-LG), were acquired in control dogs. Pre-contrast fat-suppressed T1-weighted FLAIR and heavily T2-weighted images were acquired in patient 4 and 5, respectively. For interstitial MR-LG, T1 FLAIR sequences were repeated following intradermal injection of 1.0mL Magnevist® (gadopentetate dimeglumine) into the digits of the affected limb, followed by digital massage.

***Results*:** In patients 1-3, normal lymphatic anatomy was identified in both forelimbs. There was excellent conspicuity and contrast filling of the lymphatics. Lymphatic efferent vessels and regional lymph nodes were well differentiated from local blood vessels. Partial lymphatic obstruction, collaterals, lymphedema, and severe superficial cervical lymphadenopathy were identified in patient 4. Patient 5 had well delineated lymaphatics distal to the elbow, but had lymphedema of the entire limb with extension into the mediastinum. Image mis-registration compromised the MR-LG exam in the proximal limb.

***Discussion/Conclusion*:** MR-LG provides detailed global lymphatic anatomy with superior contrast resolution. The procedure is safe, minimally invasive and can be performed in a single MR examination. The concurrent use of gadolinium enhanced T1- and heavily T2-weighted sequences in MR-LG exam is important for the assessment of severity and complete lesion delineation. Further study of normal and abnormal cases with larger numbers would be needed to validate the superior sensitivity and specificity that has been realized in human MR-LG.

RELIABILITY OF SAGITTAL T2-WEIGHTED ALONE OR COMBINED WITH SINGLE-SHOT FAST SPIN ECHO SEQUENCES FOR DETECTING SITES OF DISC HERNIATION IN 120 DOGS.

R. Guillem, J. Suran, A.V. Caceres, J.A. Reetz, W. Mai. From the University of Pennsylvania, Philadelphia, PA 19104.

Introduction/Purpose: MRI is commonly used to diagnose intervertebral disc herniation (IVDD) in dogs. To increase MRI throughput and reduce anesthesia time it is necessary to shorten acquisition times. It is common to locate areas of suspected compression on sagittal series and then obtain limited transverse series in these areas. However it is not known how accurate this method is in correctly identifying sites of significant compression and if significant compression can be missed using this step-by-step approach. The objective of this study was to assess the reliability of sagittal T2-Weighted (T2-W) series alone or in combination with a single-shot fast spin echo sequence in correctly identifying site(s) of significant cord compression due to disc herniation in a series of 120 dogs.

Methods: 120 dogs with IVDD diagnosed by means of MRI were included. All dogs had a complete MRI examination including T2 and T1-weighted sagittal and transverse series through the entire segment of interest (C1-T2, T3-L3 or L4-Sacrum). Three readers blinded to the final diagnosis were only provided with the sagittal T2-weighted (T2W) series and a Single-Shot Fast Spin Echo (SSFSE) slab for each case. The readers were asked to look at the T2W sagittal series only first, identify all sites of compression, and identify the major compression sites. The experiment was then repeated adding the SSFSE slab to the assessment. Results were compared to the final MRI report which had been generated by a radiologist with all series available including transverse series through the entire segment of interest. Complete agreement was considered when the suspected sites of compression from the sagittal series matched exactly the final report. Partial agreement was considered when the suspected sites of compression were immediately adjacent to the actual sites of compression. Differences between the three spinal segments were assessed.

Results: When focusing at only the major compressive sites, the T2W series was completely accurate in 88.3% and the T2W combined with SSFSE was completely accurate in 91.1% of cases. The T2W series was completely or partially accurate in 95.8% of cases and when adding the SSFSE slab, this increased to 96.1%. Accuracy was better for the C1-T2 segment and worse for the L4-Sacrum segment.

Discussion/Conclusion: Actual sites of compression are most of the times correctly identified from examination of a sagittal T2W series. Reliability is slightly increased by examination of a SSFSE slab. However in a small percentage of cases the actual compressive sites may not be identified accurately from the sagittal series alone, especially in the L4-S segment.

A PROTOCOL AND EARLY EXPERIENCE WITH MAGNETIC RESONANCE IMAGING FOR PERICARDIAL DISEASE AND CARDIAC MASSES IN DOGS.

Fischetti AJ, Trafny D, Fox PR. Animal Medical Center, New York, NY 10065.

Introduction/Purpose: In people, evaluation of suspected or known cardiac masses is a frequent source of referral for cardiac magnetic resonance imaging (cMRI). These masses are either incompletely imaged with echocardiography or are suspected 'pseudomasses', requiring further testing to confirm their insignificance. Current computed tomography (CT) technology has lessened the initial advantages of multi-planar cMRI, particularly with regards to cardiac function. However, cMRI remains the gold standard for comprehensive imaging of cardiac structure in pericardial diseases and cardiac masses. The purpose of this study was to establish a protocol for cardiac imaging in normal dogs and apply this protocol to dogs with echocardiographic evidence of a cardiac mass or pericardial effusion.

Methods: Three echocardiographically normal dogs had MR imaging of the skull or vertebral column. With owner and institutional consent, the scan times were prolonged to develop preliminary imaging protocols for cardiac imaging. All MR images were obtained with a 1.5 T Philips *Achieva*. Long/short-axis, transverse, sagittal, and dorsal scan planes were obtained from scout images of the heart. Pulse sequences included turbo spin echoes (T1- and T2-weighted), echo-planar imaging (EPI), cine imaging, and steady-state free precession (SSFP). Modifiers to the spin echo sequences included fat suppression and black blood techniques. The various sequences and planes were evaluated for anatomic detail and acquisition time. These techniques were applied to 11 dogs with echocardiographically-diagnosed pericardial effusion and/or cardiac masses.

Results/Discussion: Long- and short-axis planes were discontinued in favor of the more easily acquired transverse, sagital, and dorsal planes. T2-weighted images with and without fat-saturation techniques provided the most anatomic detail. Black blood techniques produced confusing high signals at the margins of heart chambers where blood flow was static. All echocardiographically-diagnosed cardiac masses with pericardial effusion were identified with cMRI. Cine imaging in systole and diastole allowed for evaluation of attachment site of cardiac masses. Images provided a global picture of cardiac masses relative to surrounding structures, aiding surgical approach. All echocardiographically-diagnosed pericardial effusions without cardiac mass were confirmed with cMRI. A possible mass identified on echocardiogram was deemed normal on cMRI. A dilated cardiac chamber noted on echocardiogram was diagnosed as an aneurysmic right auricle/atrium on cMRI. Two high signal foci in the left ventricular wall were noted in a dog with right atrial hemangiosarcoma. These were presumed cardiac metastases but were not confirmed histologically. cMRI techniques may prove useful in confirming idiopathic pericardial effusions and cardiac non-lesions, and in providing a global picture of large cardiac masses to determine extent of disease, surgical approach, and regional metastasis.

IMAGING OF CORONARY ARTERIES USING 64-SLICE MDCT ANGIOGRAPHY IN THE DOG.

R. Drees[1], A.P. Frydrychowicz[2], S.B. Reeder[2-5], M.E. Pinkerton[6], R. Johnson[1]

[1]Department of Surgical Sciences, School of Veterinary Medicine, University of Wisconsin-Madison, Madison, WI 53706; [2]Department of Radiology, [3]Medical Physics, [4]Biomedical Engineering and [5]Medicine, School of Medicine and Public Health, University of Wisconsin-Madison, WI 53792; [6]Department of Pathobiological Sciences, School of Veterinary Medicine, University of Wisconsin-Madison, Madison, WI 53706.

Introduction/Purpose: Workup of suspected obstructive coronary artery disease in people has been largely facilitated by the introduction of cardiac-gated multi-detector computed tomography (MDCT), enabling noninvasive coronary arterial computed tomography angiography (CCTA). In canine patients catheter angiography remains the current gold standard for coronary artery angiography, which is an invasive and expensive procedure. Goal of this study was to test the feasibility of state-of-the-art 64-slice MDCT as a non-invasive technology for visualization of canine coronary arteries.

Methods: Four one-year old purpose bred research dogs underwent coronary arterial angiography using 64-slice MDCT (all experiments approved by responsible IACUC). Scan of the heart was initiated following individualized delay after contrast bolus injection using helical scan mode at 120kV, ECG-modulated tube current (200-750mA), 0.35sec gantry rotation time (effective temporal resolution 250msec) using SnapShot Segment feature, (GE Healthcare, Waukesha, WI), 0.625mm collimation, 0.625mm helical reconstruction interval utilizing all 64 detectors and retrospective ECG gating. After completion of a related study all dogs were humanely sacrificed and underwent gross necropsy. The coronary arteries were evaluated for visibility and their relation to other cardiac anatomical structures. Results were compared to gross necropsy findings and references given in standard textbooks of veterinary anatomy.

Results: In all dogs accurate visualization of the left and right canine coronary arteries, their respective branches and relation to the cardiac structures were achieved using CCTA. Gross necropsy and standard anatomical descriptions matched in vivo canine CCTA findings.

Discussion/Conclusion: 64-slice MDCT canine coronary CTA presents an excellent noninvasive alternative for coronary angiography in canine patients.

This project was funded by the Companion Animal Fund of the University of Wisconsin-Madison.

LABELING OF EQUINE UMBILICAL CORD BLOOD-DERIVED MSCs WITH SPIO CONTRAST MEDIUM AND IN VIVO DETECTION WITH MRI.

R Cruz – Arámbulo,[1] P Foster[2], DH Betts[1,3], TG. Koch, [1,4]

(1) University of Guelph, Ontario, Canada N1G2W1 (2) Imaging Research Laboratories, Robarts Research Institute, London, Ontario, Canada N5X4K8 (4) University of Western Ontario, London, Ontario, Canada N6G 1G9 (3) Orthopaedic Research Lab. Aarhus University, Denmark

Introduction/Purpose: Superparamagnetic iron oxide (SPIO) is a contrast medium that has been widely used to label different kind of mesenchymal stem cells and pluripotential cells to track the in vivo location of the labeled cells once administered to an animal model. Labeled mesenchymal cells have been also used in humans and canine. The purpose of this study is to evaluate labeling efficiency of equine umbilical cord blood-derived multipotent mesenchymal stromal cells (eCB-MSCs) with 2 different SPIO particles, the effects of the 2 SPIO contrast media on cell viability and the ability to detect SPIO-labeled eCB-MSCs in vivo with MRI.

Methods: eCB-MSCs labeling was compared using two different dual modality (MRI and fluorescence) imaging agents: an ultra-small iron oxide (USPIO, 35nm) (Molday ION-Rhodamine B, BioPal) and a micron-sized iron oxide (MPIO, 0.9 μm) (Bangs Beads, Bangs Laboratories). eCB-MSCs were labeled with 100 μg Fe/mL of USPIO or 10μL/mL of MPIO (representing $5x10^8$ beads) at a concentration of 2 million cells per 4 mL by co-incubation, for 24-36 hours. Viability after labeling was assessed by the trypan blue exclusion assay. Labeling efficiency was assessed by examining cytospin slides stained with Perl's Prussian Blue (PPB); the percentage of labeled cells was determined by counting cells with and without blue staining. The distribution of USPIO in eCB-MSCs was also visualized by fluorescence imaging. For *in vivo* MRI, 1 million and 0.5 million USPIO labeled eCB-MSCs were injected SQ into the right and left flank, respectively, of a male nude mouse. Scans were performed using a clinical 3T MRI system.

Results: eCB-MSCs were labeled with USPIO and MPIO by simple co-incubation. Viability was 90.5% in unlabeled, 80% in USPIO labeled and 85% in MPIO labeled ESC. Labeling efficiency was 99% with USPIO and 90% with MPIO. The iron content per cell was much greater with USPIO. MR axial plane image of the mouse at the level of the prostate demonstrate a focal area of hypointensity in the left flank and a smaller area on the right flank. This hypointensity represents USPIO labeled eCB-MSCs distributed within the SQ tissue. The difference in the size between the two areas is probably related to the smaller amount of cells injected in the right left flank.

Discussion/Conclusion: This is the first report of the labeling and imaging of eCB-MSCs. Labeling was easily achieved by simple co-incubation and had high labeling efficiency, iron content and cell viability. eCB-MSCs were better labeled with the smaller imaging agent. Labeled eCB-MSCs were detected in vivo after injection into the mouse flank. These experiments set the stage for our future work, which will focus on effect of SPIO on cell differentiation, compare USPIO and MPIO for in vivo imaging, and tracking the location of eCB-MSCs in horses after injection in a tendonitis model.

MRI FINDINGS IN THE EQUINE STIFLE OF THE PERFORMANCE HORSE AND CORRELATION WITH THE HUMAN KNEE.

A.L. McKnight[1], K.E. Kreider[2], C.A. Dolinskas[3], J.C. Posh[4], H.T. Stevens[2], S.D. Bennett[5]
McKnight Insight, PA 19317[1]; Equine Services, FL 33414[2]; Pennsylvania Hospital, PA 19107[3]; Univ. of Pennsylvania, PA 19104[4] Equine Services, KY 40067[5]

Introduction/Purpose: The equine stifle has not previously been amenable to imaging with magnetic resonance imaging in the live performance horse due to size constraints of the horse and the gantry. Although MRI of the stifle in the live horse has previously been reported using an ultra short, wide bore 1.5T magnet (Siemens Espree), clinical exams are not typically performed due to the difficulty in positioning the horse. We report the MRI findings in 12 clinical performance horses following MRI examination of the stifle using a 0.25T MRI system. The lesions were compared to those seen in the human knee.

Methods: Twelve clinical horses (ages 2-14) were identified that had undergone MRI examination of the right or left stifle at either Equine MRI of Palm Beach in Wellington, FL or Equine Services Surgical Hospital in Simpsonville, KY from April 2008 through March 2010, including 6 Warmbloods, 3 Quarter Horses, 1 Thoroughbred, 1 Standardbred, and 1 Morgan horse. All examinations were performed on an Esaote 0.25T Rotating Vet MR Grande. The magnet was rotated 90^{o} so that the bore was vertical. All horses were scanned under general anesthesia in lateral recumbency with the hind limb of interest extended vertically so the femorotibial joint was in the magnet isocenter. A flex coil was wrapped around the dorsal aspect of the stifle. For most horses, the MRI protocol included PD- and T2-weighted sequences, STIR, and isotropic 3D GE T1 sequences. The MRI abnormalities were described, and similarities to the human knee were found for comparison purposes.

Results:

All horses had evidence of meniscal damage--predominantly one or several discrete tears, but also significant degeneration. All horses also had signal abnormalities associated with one or several of the meniscotibial ligaments. 11/12 horses had visible evidence of osteoarthritis. Additional lesions included femoral and tibial cyst-like lesions, other subchondral and bone marrow lesions, and signal changes within the cranial and caudal cruciate ligaments, medial collateral ligament, and origin of the peroneus tertius/long digital extensor tendon. Several horses also had floating tissue fragments and evidence of effusion. The abnormalities were more similar to common findings in human knees with degenerative lesions rather than acute knee trauma.

Discussion/Conclusion: Clinical evaluation of the equine stifle is possible in the performance horse using an Esaote 0.25T Rotating Vet MR Grande MRI system. In general, multiple soft tissue and bony lesions were identified that were more similar to degenerative changes in human knees rather than changes seen in acute athletic knee traumas.

CROSS-SECTIONAL PATHOLOGY AMENDS CROSS-SECTIONAL IMAGING.

S. Kneissl, A. Fuchs-Baumgartinger, A. Probst. University of Veterinary Medicine, Vienna, Austria, A 1210.

Introduction/Purpose: Exenteration, macroscopic evaluation, selective histology, and limited documentation (in text and image) characterize the standard procedures of necropsy. Ideally, volumes of tissue rather than isolated pieces should be used to compare pathologic findings to cross-sectional images. Information gained by macroscopic examination of surfaces or by high resolution microscopy complements rather than explains the appearances on cross-sectional images. To demonstrate the diagnostic advantage of necropsy based on anatomic sections, three animals that had cross-sectional imaging of the head were selected.

Methods: Two dogs and one cat with intracranial lesions seen in CT or low-field MR images were euthanized and their heads frozen. Transverse slices in the same plane as cross-sectional images were cut and photographed. Histologic sections and plastic-embedded sections were acquired and compared to cross-sectional images macroscopically, mesoscopy (using a magnifying glass), and microscopically.

Results: Both dogs had extracranial neoplasms with intracranial extensions: a 1-year, female Rottweiler had a nasal, an 11-month, female Cane Corso had a cervical undifferentiated sarcoma. The 11-year, female European Shorthair cat had an intracranial meningioma. Examination of plastic-embedded sections using magnifying glass facilitated observation of focal neoplastic infiltration, expansive growth pattern, atrophy, displacement or involvement of adjacent tissue, including meninges, cerebral layers, and vessels.

Discussion/Conclusion: Communications between radiologist and pathologists are frequently flawed because of the different methods they use to view the patient, and questions not asked specifically before necropsy might not be answered after. Since imaging findings are mostly non-specific in regard to histology, the radiologist must concentrate on gross features such as the location and extent of pathology. Between microscopy and macroscopy, mesoscopy enables a pathologic assessment that corresponds well with cross-sectional imaging features, and is likely to provide answers to questions posed by the radiologist. It is recommended that specimens of selected clinical cases are conserved in order to create an archive of clinically relevant material that complements cross-sectional imaging findings.

CT EVALUATION OF OBLIQUE SPINOUS PROCESSES IN DOGS AND CATS.

S. Kuzmits, C. Semeliker, A. Probst, A. Tichy, S. Kneissl. University of Veterinary Medicine, Vienna, Austria, A 1210.

Introduction/Purpose: Inclination of spinous processes in the sagittal plane is normally craniad or caudad depending on the vertebra. Lateral inclination is not a normal anatomic feature yet right or left inclination of thoracic and lumbar spinous processes has been observed as an incidental finding in computed tomography (CT) scans. The aims of this study were to describe the anatomic locations and prevalence of laterally inclined spinous processes in the dog and cat, and to look for associations with age or gender.

Methods: The archive of Diagnostic Imaging, University of Veterinary Medicine Vienna, was reviewed for dogs (C.S.) and cats (S.K.) that had CT scans of thoracic and lumbar vertebrae with normal and abnormal results. Spinous processes were examined in transverse images and recorded as (A) normal (tip of the spinous process in the median plane) or (B) oblique (tip of the spinous process lateral to the median plane). Associations between oblique spinous process and age, gender were analyzed using unpaired t-test and chi-squared test, respectively.

Results: 295 CT scans of dogs and 214 CT scans of cats were reviewed. Crossbred:purebred ratio for dogs was 1:3 and for cats was 1:5. Mean age of patients was 8 years (range 4 months to 18 years). Prevalence of oblique spinous processes was 21% at L5 in dogs and 12,6% at L6 in cats. Further, shape variations, such as bipartite, undulated or curved spinous processes, were observed rarely. Evaluation of spinous processes cranial to T11 was compromised by spinous process angulation resulting in a limited number of CT slices showing the spinous process and the vertebral body in one plane. No association between oblique spinous processes and age or gender.

Discussion/Conclusion: CT is an excellent modality for assessment of spinous process anatomy, provided reconstruction algorithm and slice inclination are optimized. In this study, difficulties in grading cats compared to dogs could result from a lower grade of lateral inclination and smaller size of the spinous process. In theory, chronic musculoskeletal disease could result in asymmetric muscular traction or posture. For example, spasm of the m. multifidus, a segmental muscle that extends from the mammilary, transverse, or articular processes of the caudally lying vertebrae to the spinous processes of the cranially lying ones, could act on the spinous process to favor obliquity. Alternatively, obliquity of the spinous processes may represent an anatomic variant of no clinical significance.

SUSCEPTIBILITY ARTIFACTS DUE TO METALLIC FOREIGN BODIES IN SMALL ANIMAL MRI.

S.Hecht, W.H.Adams, J.Narak, W.B.Thomas
Department of Small Animal Clinical Sciences, University of Tennessee College of Veterinary Medicine, Knoxville, TN, USA

Introduction/Purpose: Susceptibility artifacts due to metallic foreign bodies may interfere with interpretation of MRI studies. Purpose of this study was to investigate frequency and diagnostic implications of susceptibility artifacts in small animal patients presented to a Veterinary Teaching hospital in East Tennessee.

Methods: All MRI studies performed in dogs and cats over an 18-month period were evaluated retrospectively for the presence of susceptibility artifacts associated with metallic foreign bodies. Radiographs were evaluated if available to determine nature of the metallic foreign material. Severity of artifacts was graded as 0 (no interference with area of interest), 1 (extension of artifact into area of interest without impairment of diagnostic quality), 2 (impairment of diagnostic quality but diagnosis still possible) and 3 (non-diagnostic study).

Results: Artifacts were observed in 64/564 (11.3%) of MRI studies [thorax 2/3 (66.7%), cervical spine 33/130 (25.4%), musculoskeletal system (6/26; 23.1%), abdomen 1/5 (20.0%), thoracic spine(19/112; 17.0%), lumbosacral spine (1/57; 1.8%), head/brain (2/231; 0.9%)] and were caused by ID microchips (n=58), bullet fragments or shot (n=2), skin staples/suture material (n=2), ameroid constrictor (n=1) and surgical implants (n=1). Severity of artifact was grade 0 (n=29), grade 1 (n=21), grade 2 (n=11) and grade 3 (n=3).

Discussion/Conclusion:
Although susceptibility artifacts due to metallic foreign bodies are common in small animal MRI, they rarely result in non-diagnostic studies.

MAGNETIC RESONANCE IMAGING OF THE FELINE HIPPOCAMPUS.

Francis KA, Drost WT, Schmalbrock P, Burns P, Buffington CAT. The Ohio State University, Veterinary Medical Center and Wright Center of Biomedical Innovation, Columbus, OH 43210.

Introduction/Purpose: The human hippocampus is one of the more structurally discrete structures of the limbic system. Atrophy of the hippocampus secondary to high physiologic levels of cortisol has been documented. Humans exposed to chronic stress or pain, most notably patients with posttraumatic stress disorder and chronic pelvic pain syndrome, have detectably smaller hippocampal structures. Functional MRI is used to detect changes in metabolism in various areas of the brain parenchyma is a very sensitive indicator of brain function secondary to chronic pain or stress. However, functional MRI is not a viable option at this time in veterinary medicine. Feline interstitial cystitis (FIC) is a spontaneous animal model for interstitial cystitis (IC), and IC is a chronic pain syndrome in humans. Because both IC and FIC occur in patients of various ages, appear spontaneously and may remit regardless of treatment, studying brain changes in cats may aide in investigation of this chronic pain syndrome in humans. The aim of this study is to evaluate the feasibility of using structural MRI in determining changes in volume of the hippocampus in a fixed feline brain.

Methods: The study has OSU IACUC approval. Brain MRI of two, non-symptomatic cats with FIC were performed using 3 Tesla (3T) and 7 Tesla (7T) magnets. Using the 7T magnet, T2W images were made with a quadrature human knee coil (1.8mm in thickness with 0.0mm spacing) and a smaller surface (eye) coil (1.0mm and 0.5mm with 0.0mm spacing). Using the 3T magnet, T2W images were made using an 8-channel knee coil (1.8mm thick, 0.0mm spacing). Transverse, sagittal, and dorsal plane images were acquired. After induction of anesthesia, cats were imaged in vivo using the 7T and then 3T magnets, after which they were euthanized and the brains formalin fixed by perfusion. Images were acquired using the 7T and 3T magnets after perfusion fixation, in situ, after which the brains were removed and placed in 10% formalin solution. Cat 1 was imaged on days 13, 22, and 103 days post euthanasia. Cat 2 was imaged on days 13, 22, and 97 days post euthanasia. DICOM images were imported into ImageJ. The images were calibrated to a known length and regions of interest were drawn around the hippocampus in each slice that contained hippocampal tissue. Regions of interest (ROI) were traced around the area of the hippocampus on the transverse, sagittal and dorsal plane images. The areas were then multiplied by the image thickness (including spacing) and the area from each slice was summed to obtain a volume.

Results: The effect of fixation on the hippocampus volume has not been determined. There has been a large amount of variance within the measurements of the hippocampus. Measured volumes range from 150-460 mm^3. Volumes are larger on the transverse images when compared to the sagittal and dorsal images.

Discussion/Conclusion: Measurement of the feline hippocampus volume is currently difficult. The eye coil (7T) used in this study may be of use, however this coil can only be used in ex vivo brains. Further definition of the hippocampal anatomy will likely be needed as well as comparison to pathologic specimens.

EVALUATION OF ERGONOMIC RISK FACTORS AMONG VETERINARY SONOGRAPHERS.

E.K. Randall, D.P. Gilkey, A.A. Patil, J.C. Rosecrance, D.I. Douphrate. Colorado State University, Fort Collins, CO, 80526.

Introduction/Purpose: Veterinary sonographers are exposed to many of the same risk factors as their counter parts in human medicine and as a result may be at risk of developing musculoskeletal symptoms. Over 400 board certified veterinary radiologists and a large number of internists, surgeons, non-board certified veterinarians, and technicians perform diagnostic ultrasonography. The purpose of the study was to investigate the prevalence of musculoskeletal symptoms (MSS) and ergonomic risk factors among this highly specialized population.

Methods: A fifty-nine item survey was developed based upon knowledge and experience of a veterinary radiologist, ergonomic expertise of multiple faculty members, and epidemiological evidence about MSS from the literature. The survey was published online using a web based survey tool with notices emailed to 1486 veterinary sonographers including veterinary radiologists, small animal internists, cardiologists and technicians. Data were coded and analyzed using SPSS Version 18. Data were evaluated and proportions and descriptive statistics were generated. Additional analysis will look at odds ratios in relation to MSS and reported musculoskeletal disorders as outcomes.

Results: The mean age of respondents was 42 years and 56% were members of the American College of Veterinary Radiology. Survey results revealed 63% of the respondents had at some point experienced musculoskeletal related pain due to ultrasound related activities and 34% had sought medical care. Fifty-two percent reported having experienced pain while scanning and 51% experienced pain after scanning. The most frequently reported symptomatic area was the hand and wrist (12.1%) followed by the shoulder and upper arm (7.1%). Low back pain, numbness and tingling were the next most frequently reported symptoms, (2.1%) respectively. However, a large majority (73.8%) reported more than one symptom. Of all the respondents, 83% were Veterinary Radiologists or Internal Medicine specialists with 47% practicing ultrasonography for nine years or less. Of the three strenuous areas to examine, 45.5% reported the abdomen as the most difficult followed by thorax at 27.5% and limbs at 21.7%.

Discussion/Conclusion: Early analysis of data suggests that veterinary sonographers suffer from a high prevalence of MSS. Further analysis of the data will include odds ratio estimates for risk assessment. Investigators plan to evaluate the relationship of work exposures to MSS. The next phase will be to evaluate exposure assessment using ergonomic tools and methods and ultimately develop interventions to reduce the burden of MSDs among veterinary sonographers.

LACK OF ASSOCIATIONS BETWEEN ULTRASONOGRAPHIC APPEARANCE OF THE CANINE LIVER AND HISTOLOGIC DIAGNOSIS. C.M.R. Warren-Smith, S. Andrew S, C.R. Lamb. The Royal Veterinary College, University of London, Hertfordshire AL9 7TA, U.K.

Introduction/Purpose: Although the liver is routinely examined ultrasonographically, morphologic features do not enable specific diagnosis. Certain lesions have been associated with specific diagnoses (e.g. target lesions with malignancy), but definite diagnosis requires histology. The aim of this study was to reassess if there are any ultrasonographic features that may enable tentative diagnosis when histology is pending or when managing patients in which liver biopsy is considered inappropriate.

Methods: Hospital records from 1999-2009 were searched for dogs that had abdominal ultrasonography and subsequent liver biopsy or necropsy within 7 days. Ultrasound reports were retrieved and the liver categorized as normal or abnormal and the appearance of lesions by distribution, echogenicity, presence of target lesions, presence of a cavitary lesion, cyst or calcified material, liver size, surface contour, and presence of peritoneal fluid. Histologic diagnosis was recorded. Cases were excluded when liver histology was normal or inconclusive, when patient records were incomplete or when diagnosis occurred in less than 4 dogs. In instances where both liver biopsy and necropsy results were available, the necropsy results were used preferentially.

Results: Records of 371 dogs with 15 different hepatic diagnoses satisfied the inclusion criteria. Histologic diagnoses were hepatitis (n=77), nodular hyperplasia (n=47), vacuolar change (n=45), fibrosis (n=32), primary hepatic carcinoma (n=30), lymphoma (n=28), metastatic neoplasia (n=27), necrosis (n=21), lipidosis (n=17), hemangiosarcoma (n=13), round cell tumors (n=9), hepatocellular adenoma (n=8), degenerative change (n=6), steroid hepatopathy (n=7), and extramedullary hematopoiesis (n=4). Sensitivity of ultrasonography varied from 86% for steroid hepatopathy to 48% for hepatitis. Ultrasonography had sensitivity of 73% for primary hepatic neoplasia and 56% for hepatic metastasis. Marked variability in ultrasonographic appearance of lesions was observed for all diagnoses. Testing using multivariable classification tree analysis was attempted, but proved impossible because of insufficient power for this number of diagnoses, hence no significant associations between ultrasonographic appearance and diagnosis were found. Various possible trends were noted: 5 (71%) livers with steroid hepatopathy and 7 (46%) livers with lipidosis were diffusely hyperechoic; in 12 (67%) instances target lesions were malignant; 8 (62%) dogs with hepatic hemangiosarcoma had peritoneal fluid in addition to hepatic lesions; 52 (59%) livers with primary neoplasia and 24 (51%) livers with nodular hyperplasia had multifocal or diffuse lesions on ultrasonography.

Discussion/Conclusion: Ultrasonography is an insensitive test for hepatic disease in dogs. When the liver appears abnormal ultrasonographically, the marked overlap in the appearance of different hepatic conditions will prevent tentative diagnosis. Histologic examination remains essential for diagnosis of canine hepatic disease.

DIAGNOSTIC VETERINARY IMAGING USING MICRO-IMAGING PLATFORMS.

J. S. Wall, A. Stuckey, S. J. Kennel, T. Richey, [1]F. Morandi, [1]M. Jones, [1]C. Greenacre, [2]M. Souza, and [1]A. LeBlanc

University of Tennessee Graduate School of Medicine, Knoxville, TN; [1]Departments of Small Animal Clinical Sciences and [2]Comparative Medicine, University of Tennessee College of Veterinary Medicine, Knoxville, TN, 37922.

Introduction/Purpose: Functional and anatomic imaging techniques such as positron emission (PET) and x-ray computer tomographies (CT), respectively, have revolutionized the practice of medicine by providing non-invasive methods to detect pathology and monitor the progression and regression of disease. PET imaging of ^{18}F-fluorodeoxy glucose (^{18}FDG) has provided a rapid and quantitative means of monitoring response to therapy that provides early feedback to the physician enabling expeditious changes in the therapeutic strategy to benefit the patient. These same advantages are also available to veterinarians who evaluate animal images acquired on human clinical CT, MRI, and PET scanners. Although the spatial resolution of these imaging platforms is adequate for diagnostic imaging of most companion animals, many smaller species such as birds, pocket pets, and small dogs and cats may benefit from higher resolution micro imaging.

Methods: We have utilized small animal imaging microCAT II, microPET P4 and Inveon tri-modality platforms to image unconventional small animals. The patients were generally anesthetized with isoflurane and image data acquired over ~ 10 min for CT or ~ 60 for whole body PET imaging. Although limited by relatively small fields of view, as compared to clinical scanners, the sub-millimeter resolution affords unprecedented detail in the images.

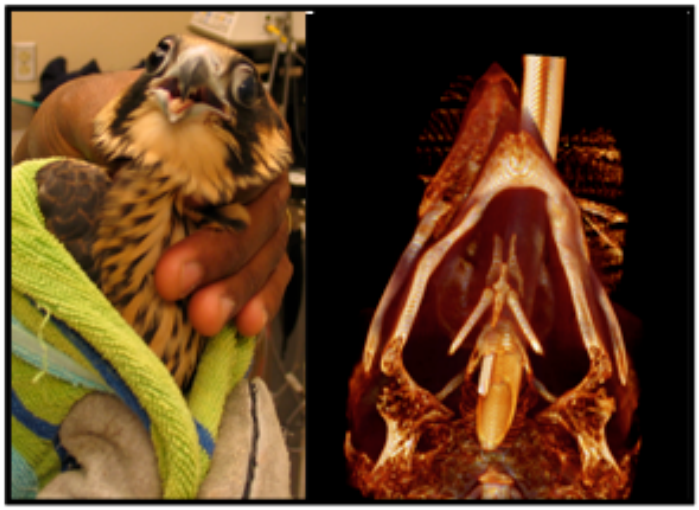

Results: Here we present anatomic studies that include a pair of male guinea pigs with osteomyelitis; various wild or client-owned avian species with skeletal abnormalities including a peregrine falcon (see microCT opposite) with a malaligned lower mandible and a cockatiel with a short, oblique, mid-diaphyseal femoral fracture; and a California King snake with a fibropapilloma.

Discussion/Conclusion: These studies demonstrate the utility of small animal imaging platforms capable of sub-millimeter resolution for diagnostic veterinary imaging of small and exotic animals. Furthermore, we have demonstrated that CT imaging of large avian species using these small FOV platforms does not result in out-of-field-of-view artifacts.

INITIAL EXPERIENCE WITH THE CLASSROOM PERFORMANCE SYSTEM™ (CPS™) IN RADIOLOGY EDUCATION.

S.Hecht[1], W.H.Adams[1], M.A.Cunningham[2], I.F.Lane[1]
[1]Department of Small Animal Clinical Sciences and [2]Instructional Resources, University of Tennessee College of Veterinary Medicine, Knoxville, TN, USA

Introduction/Purpose: Classroom performance systems (CPS) [audience response systems (ARS); "clickers"] provide a means of encouraging student interaction in a traditional didactic lecture setting. CPS™ is the leading response system in education, being used by over 5 million students worldwide. CPS™ response pads ("clickers") are handheld devices that allow students to respond to questions asked during a lecture enabling students and instructors to instantly assess their comprehension of lecture material.

Methods: Student performance in and student evaluations of the 3rd year (5th semester) didactic radiology course were evaluated from 2005 – 2009. Additionally, student interactions were evaluated subjectively by instructors who used CPS™.

Results: From 2005 – 2008, all lectures and laboratory sessions were held in conventional fashion. In 2009, CPS™ was utilized by 3/5 instructors. There was no significant difference in overall student performance and student performance on individual instructor's exam questions. On a scale from 1 (worst) to 5 (best) the radiology course was evaluated higher by students when CPS™ was used than not, however, this difference was not significant ($p=0.075$). Subjectively, students appeared more interested and involved when CPS™ was used.

Discussion/Conclusion: CPS may be beneficial in radiology education. Benefits include interactive involvement of students in a lecture setting and immediate feedback for students and instructors. Disadvantages include time constraints, technical problems and dependence on willing student participation.

American College of Veterinary Radiology

ACVR 2010 Conference Special Activities

Monday, August 16

The Vanderbilt Terrace
Reception supported by
Orthopedic Foundation for Animals
and
Universal Medical Systems, Inc.
6:30 – 7:30 p.m.

Special dedication to the memory of Dr. Myron “Mike” Bernstein